



저작자표시-비영리-변경금지 2.0 대한민국

이용자는 아래의 조건을 따르는 경우에 한하여 자유롭게

- 이 저작물을 복제, 배포, 전송, 전시, 공연 및 방송할 수 있습니다.

다음과 같은 조건을 따라야 합니다:



저작자표시. 귀하는 원저작자를 표시하여야 합니다.



비영리. 귀하는 이 저작물을 영리 목적으로 이용할 수 없습니다.



변경금지. 귀하는 이 저작물을 개작, 변형 또는 가공할 수 없습니다.

- 귀하는, 이 저작물의 재이용이나 배포의 경우, 이 저작물에 적용된 이용허락조건을 명확하게 나타내어야 합니다.
- 저작권자로부터 별도의 허가를 받으면 이러한 조건들은 적용되지 않습니다.

저작권법에 따른 이용자의 권리는 위의 내용에 의하여 영향을 받지 않습니다.

이것은 [이용허락규약\(Legal Code\)](#)을 이해하기 쉽게 요약한 것입니다.

[Disclaimer](#)

Master's Thesis

MACHINE LEARNING BASED PREDICTIVE
MODELING OF DIMENSIONAL QUALITY IN
DIRECT ENERGY DEPOSITION WITH
SUS316L

Tae-Yang Choi

Department of Mechanical Engineering

Graduate School of UNIST

2020

MACHINE LEARNING BASED PREDICTIVE
MODELING OF DIMENSIONAL QUALITY IN
DIRECT ENERGY DEPOSITION WITH
SUS316L

Tae-Yang Choi

Department of Mechanical Engineering

Graduate School of UNIST

MACHINE LEARNING BASED PREDICTIVE
MODELING OF DIMENSIONAL QUALITY IN
DIRECT ENERGY DEPOSITION WITH
SUS316L

A thesis
submitted to the Graduate School of UNIST
in partial fulfillment of the
requirements for the degree of
Master of Science

Tae-Yang Choi

06/10/2020

Approved by

Namhun Kim

Advisor

Namhun Kim

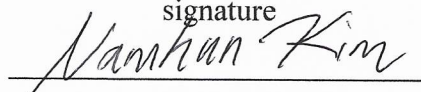
MACHINE LEARNING BASED PREDICTIVE
MODELING OF DIMENSIONAL QUALITY IN
DIRECT ENERGY DEPOSITION WITH
SUS316L

Tae-Yang Choi

This certifies that the thesis of Tae-Yang Choi is approved.

06/10/2020 of submission

signature



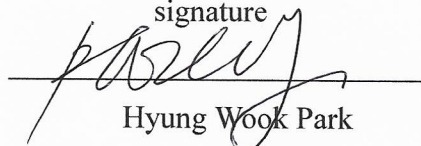
Advisor: Namhun Kim

signature



Sang Hoon Kang

signature



Hyung Wook Park

Abstract

This study aims to predict the dimensional quality of Direct Energy Deposition (DED) process on single and multi-track which are basis for the final product via machine learning. DED is a complex process of spraying powder onto a substrate and melting the material through a laser. Many process parameters (Laser power, Powder feed rate, etc.) affect output quality such as geometry (width, height, angle), mechanical properties (relative density, tensile strength, etc.). In order to see this effect, the DOE method, in which only one result is correlated with multiple factors, is used before, but machine learning is more effective in additive manufacturing in which multiple qualities needs to be predicted simultaneously.

In this study, a predictive model was generated through machine learning by using process parameters (Laser power, Powder feed rate, Coaxial gas) and dimensional qualities (Width, Height, Angle for single track, Height for multi-track) for the input and output data, respectively. After collecting the data, we trained the model using the five algorithms, Support Vector Machine (SVM), Random Forest (RF), Gradient Boosting Regression Tree (GBRT), and Artificial Neural Network (ANN), most commonly used as regression models in machine learning. After examining and comparing each generated prediction model through a goodness-of-fit test, the model generated using ANN was finally selected. When the selected model predicted the height of the multi-track most prominently, the r-square was as high as 96.63%. Afterwards, more than 4000 new datasets were created to derive optimal process parameter that met the dimensional objectives. The results are 300 W, 3.7 g/min, and 6 l/min for laser power, powder feed rate, and coaxial gas, respectively.

By using machine learning to predict output more accurately and faster than conventional methods, optimal process variables can be effectively derived in terms of time and cost. And, ultimately, it can be a cornerstone in researching future technologies that change process parameters in real time and monitor output results.

Contents

Abstract.....	i
Contents	ii
List of Figure	iii
List of Tables	iv
1. Introduction	1
1.1 Background.....	1
1.2 Research objective.....	2
1.3 Outline.....	3
2. Background research	4
2.1 Classification of metal AM.....	4
2.2 Process parameters in DED.....	6
2.2.1 Study of process parameter in SUS316L.....	8
2.3 Classification of Machine Learning Regression Algorithms	8
2.4 Previous work.....	13
3. Methodology	22
3.1 Experiment equipment and material used.....	22
3.2 Data selection	23
3.3 Data collection and post-processing.....	25
3.4 Generating predictive model.....	27
3.4.1 Predictive model of Multiple Linear Regression(MLR).....	28
3.4.2 Predictive model of Support Vector Regression(SVR)	28
3.4.3 Predictive model of Gradient Boosting Regression(GBR).....	30
3.4.4 Predictive model of Random Forest Regression(RFR).....	31
3.4.5 Predictive model of Artificial Neural Network(ANN).....	32
4. Result	34
5. Conclusion and contribution.....	37
Reference.....	39
Appendix A : MX-600 specification.....	42
Appendix B : Fatigue test result in previous work.....	42
Appendix C : Dimensional quality data from all paramters.....	43
Appendix D : Python code of Algorithms.....	48
Appendix E : Model comparison(ANN vs MLR) using scatter and plot.....	49

List of Figure

Figure 1.1 3D Printing metal market size 2014 – 2025	1
Figure 1.2 3D model of single track(a), multi-track(b), and 3d object(c).....	2
Figure 1.3 Flow of experiment.....	3
Figure 2.1 The schematic diagram of Powder Bed Fusion(PBF)	5
Figure 2.2 The schematic diagram of Direct Energy Deposition(DED).....	6
Figure 2.3 The schematic illustration of classification and regression in ML	9
Figure 2.4 Surface plot melt pool depth.....	9
Figure 2.5 The schematic illustration of support vector regression	10
Figure 2.4 Single regression tree.....	11
Figure 2.5 Structure of Artificial Neural Network(ANN).....	12
Figure 2.6 3D model of double pipe	13
Figure 2.7 Experiment process of process parameter optimization	14
Figure 2.8 Actual deposited dimension and cross-section of single track	15
Figure 2.9 Width and Height of single track according to Laser power	16
Figure 2.10 Width and Height of single track according to powder feed rate at 350W.....	16
Figure 2.11 Width and Height of single track according to Coaxial gas rate.....	17
Figure 2.12 Actual deposited multi-track.....	17
Figure 2.13 Cross section of multi-track.....	18
Figure 2.14 Actual deposited cube specimens	19
Figure 2.15 (a)Tensile, (b)Impact, (c)Fatigue specimens of optimal parameter	20
Figure 2.16 S-N curve of fatigue test.....	21
Figure 2.17 (a)Direct energy deposition of prototype and (b)final prototype.....	21
Figure 3.1 Insstek MX-600	22
Figure 3.2 SEM image of SUS316L powder	23
Figure 3.3 The schematic illustration of support vector regression	24
Figure 3.4 Deposition of (a)single track and (b)multi-track	26
Figure 3.5 Cross section of (a)single track and (b)multi-track	26
Figure 4.1 Scatter of multi-track height between actual and predicted value in (a)ANN and (b)MLR.35	
Figure 4.2 Plot of multi-track height value in (a)ANN and (b)MLR.....	35

List of Tables

Table 2.1.1 Classification of Metal Additive Manufacturing.....	4
Table 2.2 Process parameter in DED	7
Table 2.3 Process parameter study of SUS316L in DED.....	8
Table 2.4 Value of process parameter	14
Table 2.5 Optimal process parameter of single track.....	17
Table 2.6 Width and Height of Single and multi-track according to powder feed rate at 350W,7l/min18	
Table 2.7 Dimension of cube specimens according to powder feed rate	19
Table 2.8 Relative density of cube specimens according to powder feed rate.....	19
Table 2.9 Final Optimal process parameter.....	20
Table 2.10 Result of Tensile test and comparison to Castings	20
Table 2.11 Result of Impact test and comparison to Castings.....	20
Table 3.1 Particle size of SUS316L powder	23
Table 3.2 Classification and range of Input data.....	23
Table 3.3 Target value of output data.....	25
Table 3.4 Set of input data	25
Table 3.5 Formation of data	27
Table 3.6 Normalized and randomly shuffled data	27
Table 3.7 Model accuracy of MLR	28
Table 3.8 Model accuracy of SVR.....	29
Table 3.9 Model accuracy of GBR.....	30
Table 3.10 Model accuracy of RFR	31
Table 3.11 Model accuracy of ANN.....	32
Table 4.1 Comparison model accuracy	34
Table 4.2 Description of optimal predictive model.....	36
Table 4.3 Optimal process parameter from ANN predictive model.....	36

1. Introduction

1.1 Background

"In order for the manufacturing industry to survive, we need to build an AI analytics platform to improve maintenance costs and productivity," said Altmann, chief executive officer at SAS(Statistical Analysis System). The manufacturing sector, which was classified as secondary industry, changed its meaning with the advent of the fourth industry, called industry 4.0. Nowadays, the efficient management of vast data and fast decision-making determines the business of the enterprise, so the manufacturing sector also faced the reality of ‘Digital transformation’, starting with the 4th industrial revolution. This revolution is important to the existing manufacturing technology, but it is even more important for the additive manufacturing technology, which is considered an essential technology of the Industry 4.0 with the strength of multi-category small-volume production.[1]

AM is a technology that creates 3d shapes by joining layers based on 3d data. The AM is classified according to the material used, its form, and the methods of joining. In addition, since the category of materials is wide, various materials can be used[2-3]. Typical examples are plastic, ceramics, composites, metal and glass. Among them, the method of using metal is called metal AM, and this technology is applied to various industries such as automobile, aerospace, shipbuilding, and medical. According to statistics from ‘Grandviewresearch’, it can be seen that the market size of metal AM is rapidly increasing. The most popular methods of Metal AM are Powder Bed Fusion (PBF) and Direct Energy Deposition (DED), and also called Selective Laser Melting (SLM) and Direct Metal Laser Sintering (DMLS) respectively[2-3].

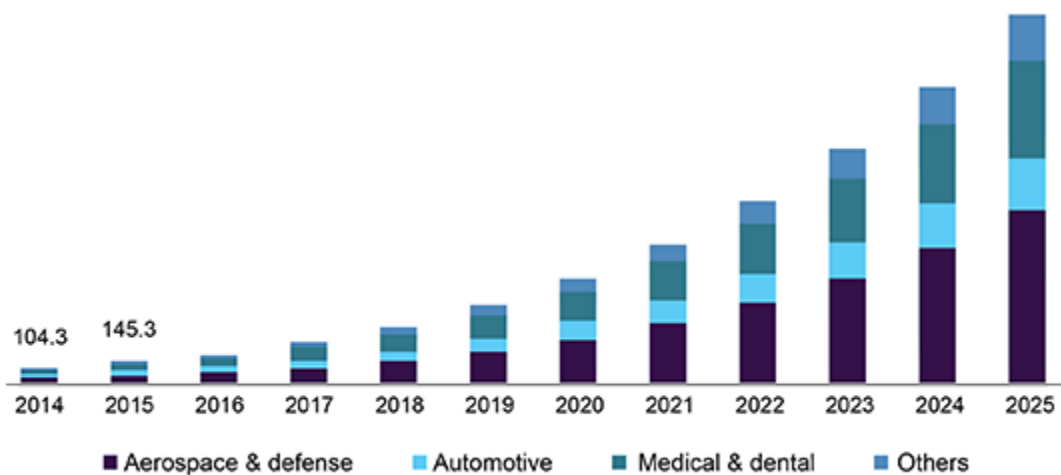


Figure 1.1 3D Printing metal market size 2014 – 2025

Since the method of Metal AM is basically a method of melting and joining metals and operating in an automated manner, it is important to set various process variables and external factors such as

internal temperature or material quality. In order to deal with such a complicated process, research using various analysis methods has been conducted.

Recently, research on applying Artificial Intelligence(AI) technology to Metal AM in connection with the 4th Industrial Revolution is actively underway. Machine Learning(ML), a sub-area of AI, trains data through algorithms based on statistics and creates models between data. Therefore, it is used in metal AM to make models for predicting the quality of defects and mechanical properties[4-6]. Popular example is to predict defects such as delamination and splatters in products by Convolutional Neural Network(CNN) images analysis using data obtained using a thermal imaging camera. There is research[7].

1.2 Research objective

The aim of study is to generate a predictive model of dimensional quality using machine learning to analyze the correlation between key process parameters and geometrical qualities. In DED process, various process parameters influence many geometrical qualities. Among them, Three key process parameters, Laser power(LP), Powder feed rate(PFR), Coaxial gas rate(CGR), were selected to conduct the experiment. Grounded on the fact that Multi-track is aggregations of single track and 3D object is aggregations of multi-track, Geometrical quality of single and multi-track is directly related to the quality of the printed product. By analyzing relationship between key process parameters and geometrical qualities of single track and multi-track, appropriate process parameters can be set according to the desired quality. Furthermore, this study can be used as a basic study in creating predictive models for dimensional quality as well as other qualities such as micro-structure or mechanical properties.

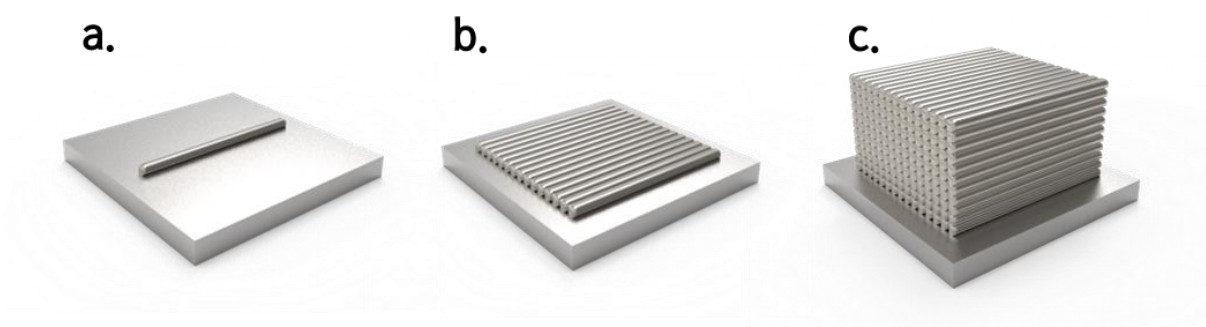


Figure 1.2 3D model of single track(a), multi-track(b), and 3d object(c)

1.3 Outline

This paper consists of a total of four chapters. Chapter 1 describes the introduction and purpose of this research. In Chapter 2, we will describe the techniques and machine learning algorithms used in the study, and previous research that motivated this study. In Chapter 3, the experimental equipment and materials used will be explained, and then the data collection method and data structure will be explained. After that, we will apply the data to the four algorithms to create a model and compare the results. After comparison, we will select the final predictive model and find the desired target process parameter. In the final chapter, we will discuss conclusions, contributions, and future work.

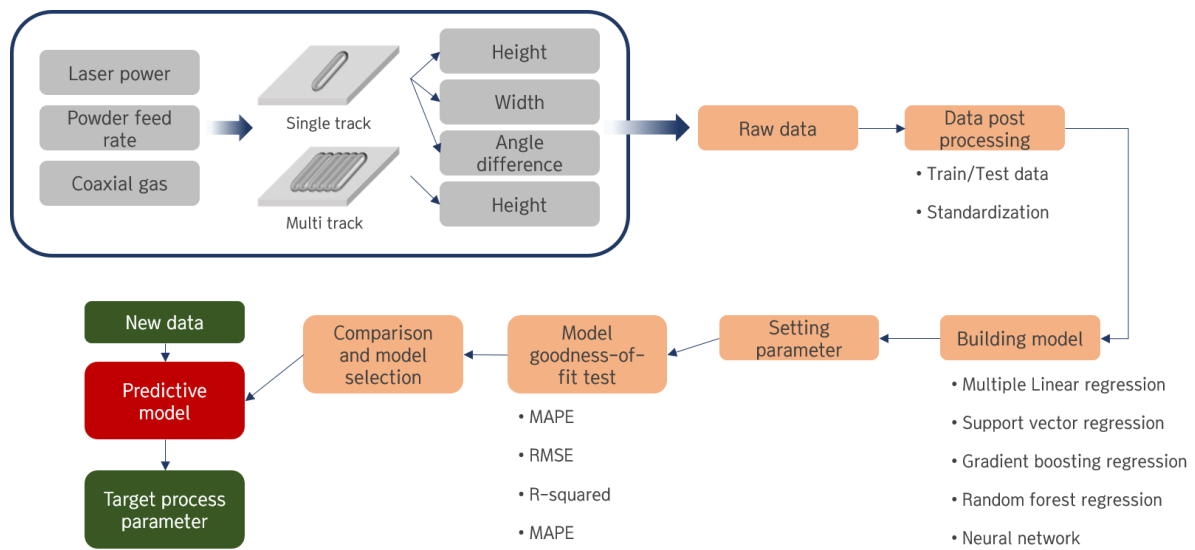


Figure 1.3 Flow of experiment

2. Background research

2.1 Classification of metal AM

In order to classify metal additive manufacturing, there are mainly three criteria. The first is how the material is prepared and based on this method, it is largely classified into Powder Bed Fusion (PBF) and Direct Energy Deposition (DED).[8]. And the other two criteria are classified according to the type of material used and the type of energy source. The type of materials used are typically powder and wire, and energy sources are laser and electron beam[9].

System	Material	Energy source	Process
PBF	Powder	Laser	Selective Laser Sintering(SLS)
	Powder	Laser	Selective Laser Melting(SLM)
	Powder	Electron Beam	Electron Beam Melting(EBM)
DED	Powder	Laser	Direct Metal Tooling(DMT)
	Powder	Laser	Direct Metal Deposition(DMD)
	Powder	Laser	Laser Engineered Net Shaping(LENS)
	Wire	Laser	Wire Laser Additive Manufacturing(WLAM)
	Wire	Plasma Arc	Wire Arc Additive Manufacturing(WAAM)
	Wire	Electron Beam	Electron Beam freeform Fabrication(EBF)

Table2.1.1 Classification of Metal Additive Manufacturing

Powder Bed Fusion(PBF)

PBF using metal powder as a material is generally divided into a place for supplying powder and a bed for supplying an energy source to melt the powder. After supplying the energy source to the powder applied to the bed and solidifying it, the bed goes down one layer, and the powder is coated with a roller again and the process of irradiating and solidification is repeated to create a 3D shape. The most popular PBF technologies are Selective Laser Melting(SLM) in which powder is melted using a Co2 laser as an energy source, and a similar method is an Electron Beam Melting(EBM) using an electron beam as an energy source.[10-12].

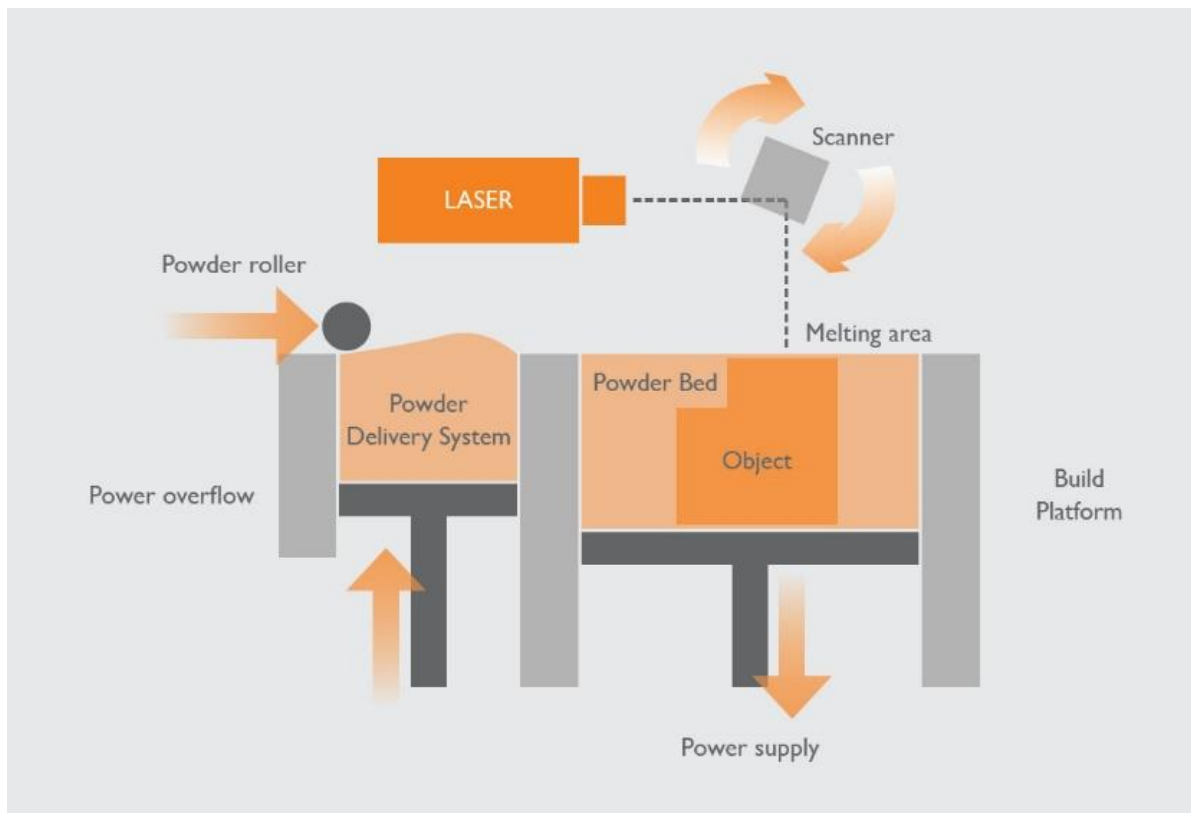


Figure 2.1 The schematic diagram of Powder Bed Fusion(PBF)

Direct Energy Deposition(DED)

In Direct Energy Deposition, a melt pool is instantaneously generated by irradiating a high-power laser beam or an electron beam onto a metal surface. At the same time, a 3d shape is produced while supplying metal powder or wire. DED technology is also classified into various types such as Direct Metal Tooling(DMT), Laser Engineered Net Shaping(LENS), Direct Metal Deposition(DMD), Electron Beam Additive Manufacturing(EBAM), and Wire Arc Additive Manufacturing(WAAM) depending on the type of material or energy source used in the same way as PBF[13-15]. The main difference from the

PBF method is that the PBF fills the powder bed with all the powder, while the DED method supplies powder or wire only to the parts to be stacked. The advantages of DED are, first of all, that metal powders used in general industries are available and there are no restrictions on the types, so the range of materials available is wide, such as Titanium, Inconel, Hastelloy, Stainless steel and Copper-Nickel alloys. In addition, it is possible to laminate with a larger area than other additive manufacturing technologies, and it is possible to manufacture with excellent mechanical quality with accurate and fine structure because the melting between materials is perfectly achieved. However, since the surface quality of the resulting product is poorer than the PBF method, there is a disadvantage that post-processing is required.

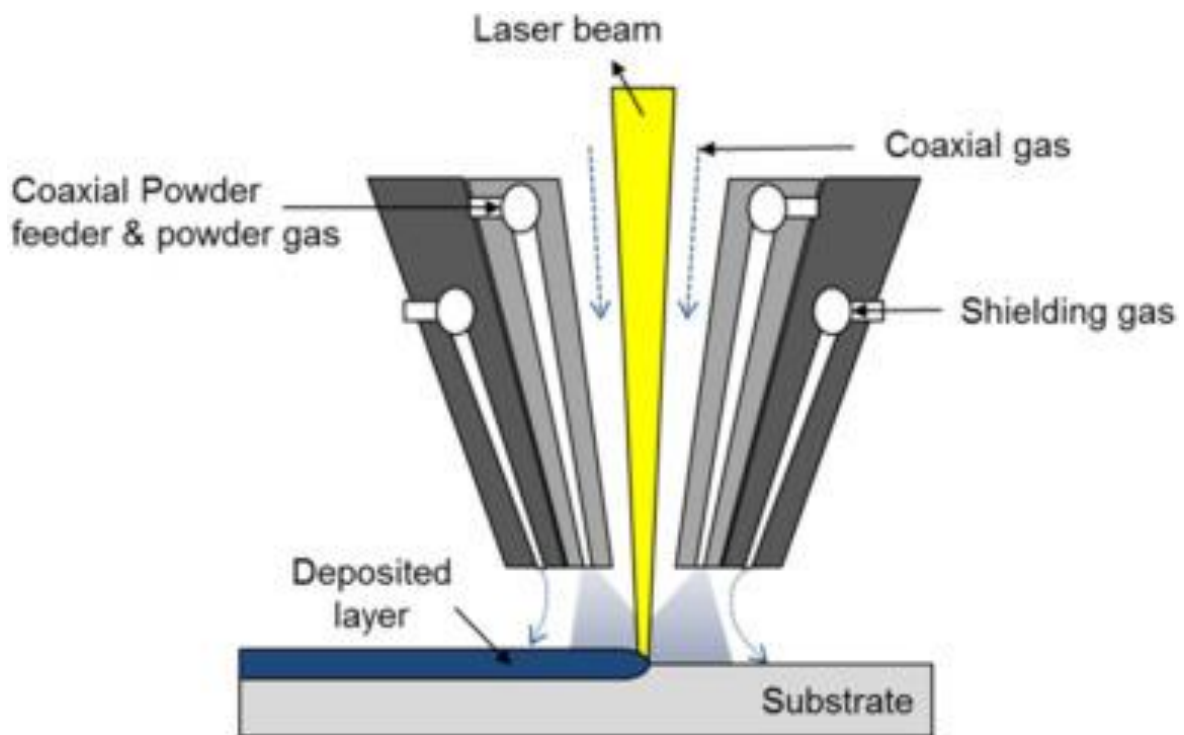


Figure 2.2 The schematic diagram of Direct Energy Deposition(DED). Reprinted permission from ref 17. © 2016 Elsevier B.V.

2.2 Process parameters in DED

In the DED process, process parameters play a very important role in creating 3d shapes. The process parameters are the input values that must be set on the machine before operating the equipment. The important variables in the DED process are laser power(LP), powder feed rate(PFR), scanning speed(SS) and coaxial gas rate(CGR). The reason process parameters are important is that they have a great influence on the quality of the manufactured product, mechanical properties, micro

structure, dimension and other qualities. The magnitude of the effect of each process parameters on the output result is also different and can vary depending on the material and the equipment used. For this reason, research on the correlation between process variables and output quality is actively underway.

Process parameter	Description
Laser power(W)	Powder is spilled from the nozzle, and a laser beam with high power is irradiated the melt the metal powder.
Powder feed rate(g/min)	The amount of powder that flows down per minute.
Scanning speed(mm/min)	the velocity of travel of a nozzle.
Hatching space(mm)	The overlapping distance between a track and a track.
Beam diameter(mm)	The diameter of the laser beam being investigated.
Coaxial gas(l/min)	It serves to spread the powder evenly with gases sprayed on both sides of the nozzle and to prevent the occurrence of plasma.
Powder gas(l/min)	Small quantities of gas used to spray powder to avoid entrapment in shafts; not affecting laminated geometry.

Table 2.2 Process parameter in DED

As an example of related research, Izadi et al. [18] divided the energy density (the product of the scan speed, hatching distance, and layer thickness divided by laser power) into a total of nine levels in the DED process to study the correlation with various qualities. The correlation between variables with dimensional quality, porosity, and compressive stiffness was studied. They concluded that it was difficult to explain the correlation with nine data.

2.2.1 Study of process parameter in SUS316L

SUS316L is an ultra-low carbon steel and has high temperature strength and excellent intergranular corrosion resistance in a welded state. For this reason, SUS316L is widely used in the metal AM field regardless of the method in powder or wire form. As shown in Table 2.3 below, it can be seen that the experiment is carried out by varying the process parameters according to the equipment used or the experiment goal. In other words, the process variable should be set differently according to the environment of use or the quality of materials, and it is important that these data are accumulated.

ref	Year	Powder	Process parameter			
		Size [μm]	Laser Power [W]	Scanning speed [mm/min]	Powder Feed rate [g/min]	Coaxial gas [l/min]
[19]	2018		300-1000	127-1143	0.9-28.8	
[20]	2019	45-150	500-900		3-9	2-8
[21]	2017		150-600	450	2.5	
[22]	2011	45-75	180-360	300-900	1.5-4.5	
[23]	2016		1280-2000	800-1250	11-18	4.8-7.5
[24]	2017	44-149	360	978	10	
[25]	2019	22-53	900	850	4.5	6

Table 2.3 Process parameter study of SUS316L in DED

2.3 Classification of Machine Learning Regression Algorithms

Machine learning(ML) can be classified into three types: supervised learning, non-supervised learning and reinforced learning. Among them, supervised learning is one of the most widely and successfully used machine learning methods. It has input and output data and is used to predict and output from a given input. Classification and regression are typical examples of supervised learning. Classification is to predict one of several predefined class labels. Face recognition, number discrimination, etc. are famous examples. The classification is divided into binary classification divided into two classes and multiple classification classified into three or more classes. Regression is the prediction of a continuous number or floating point number. This includes algorithms for predicting stock prices and making profits.[26-27]. The main difference between classification and regression is whether the results you want to predict are continuity. To apply these techniques to Metal AM, regression should be used to predict dimensional values with continuity as in the subject of this

study, and classification should be used to predict defects through images.[28]. Therefore, in order to make good use of machine learning, it is important for the user to accurately recognize the problem to be solved, determine what data to collect and refine, and choose which algorithm to use.

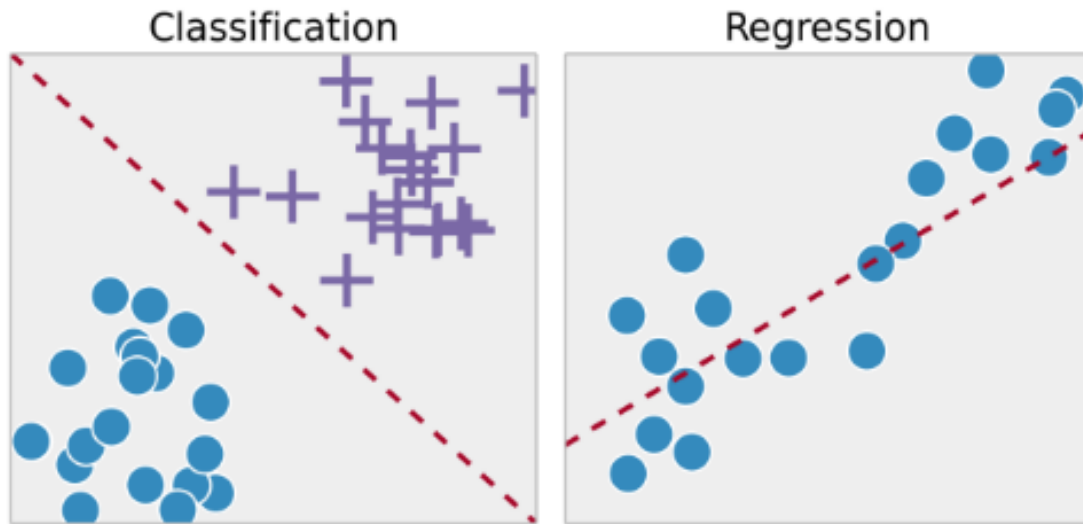


Figure 2.3 The schematic illustration of classification and regression in ML

Multiple Linear Regression(MLR)

Multiple linear regression(MLR) is an extension of linear regression that linearly expresses the relationship of the dependent variable y to the independent variable x , and linearly expresses the relationship of one dependent variable for two or more independent variables.

$$y = W_0 + W_1x_1 + W_2x_2 + \dots + W_nx_n + \epsilon$$

Cheng et al.[29] studied the correlation between process variables and depth of melt-pool through simulation of stacking thin layers of Ti-6Al-4V with Electron Beam Additive Manufacturing (EBAM) technology. After setting the scanning speed, beam power, and beam diameter as independent variables and generating a total of 64 samples, the correlation with depth was analyzed through MLR.

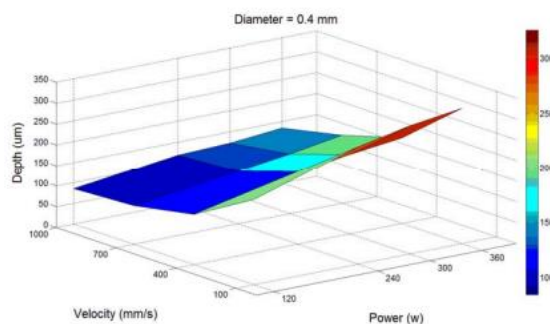


Figure 2.4 surface plot melt pool depth

Support Vector Regression(SVR)

Support Vector Machine is a machine learning method proposed by Vapnik (1996) that can solve classification or regression problems. Among them, the algorithm used when using the regression problem is called SVR. To explain SVR, you need to know the concept of Margin. You can think of Margin as a road for explaining data. In the case of classification, for example, it is to learn to maximize the width of a function generated to classify two types of data. At this time, samples located at the margins of are called support vectors. To go back to the problem of regression, regression can be thought of as the opposite of classification. In the case of classification, if the objective function is to maximize the width of the road, in the case of regression, the objective function can be set to explain the data while minimizing the width of the road. There are several hyper-parameters that must be defined to create the SVR model. First, there are Kernels that help to explain the data by converting it into a straight line by raising one dimension of the data. In addition, there are gammas that control how much the model will be affected by the dimension and C values that determine the width of the road.

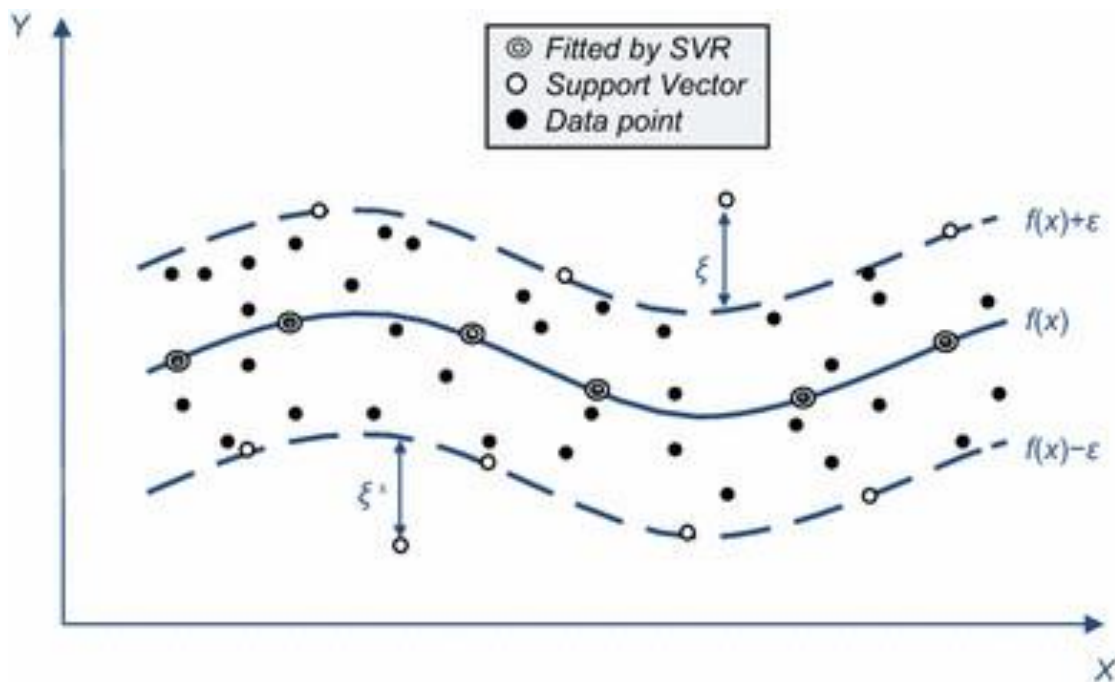


Figure 2.5 The schematic illustration of support vector regression
 Reprinted permission from ref.33 © 2020 Springer Nature Switzerland AG

Gradient Boosting Regression(GBR)

Before explaining the gradient boosting regression(GBR), I will describe the decision tree. Decision trees are an analysis method in which decision rules are represented in a tree structure to classify or predict the entire data into several subgroups. In the decision tree, the upper node is called the parent

node, the lower node is called the child node, and the node that is no longer branching is called the terminal node. It is important to select classification variables at every step of forming a tree structure from a parent node to a child node. The classification variable in the upper node is selected such that the homogeneity within the node and the heterogeneity between the nodes become the largest.

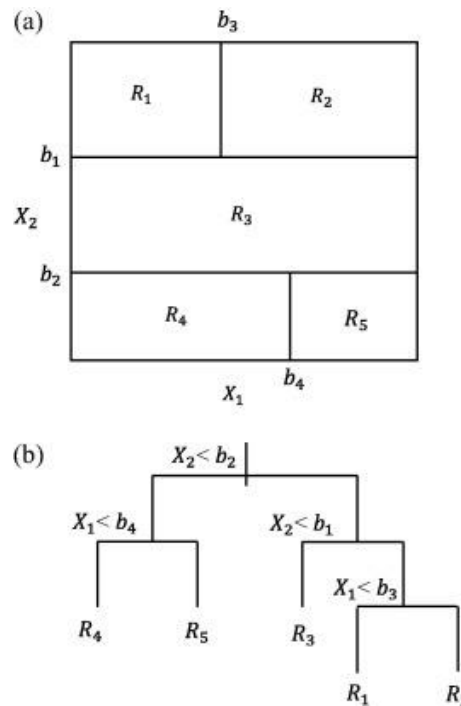


Figure 2.6 Single regression tree

Reprinted permission from ref.34 Copyright © 2015 Elsevier Ltd.

GBR is an ensemble method, one of the machine learning techniques that combines many decision trees into a powerful model. This is an algorithm that adds a new tree in the direction of reducing the error between the predicted value and the target value of the previous tree. To this end, the loss function is defined and the tree to be added next is corrected for the value to be predicted using the gradient descent method. Important parameters are `n_estimator`, which specifies the number of trees, and `learning_rate`, which controls how strongly the error of the previous tree is corrected[35]. The larger `n_estimator`, the more likely the model is to become more complex and overfitting, and the lower the `learning_rate`, the more trees need to be added to create a model of similar complexity. Therefore, it is efficient to adjust the `n_estimators` first and then find the appropriate `learning_rate`.

Random Forest Regression

Random Forest Regression (RFR) is one of the ensemble techniques, such as GBR, and is a machine learning technique that randomly mixes different decision trees to find prediction values. An important parameter is `n_estimator`, which determines the number of trees. RFR does not require data

post-processing and parameter tuning is not complicated, but its performance is excellent. So, It has been applied in various fields.

Artificial Neural Network(ANN)

An Artificial Neural Network(ANN) means a neural network artificially constructed based on the working principle of a human neuron to train a computer. Basically, one neuron receives an input (X), creates an output (Y), and delivers it to the next neuron. In practice, it is passed using an activation function to produce an effective form of output. The result of multiplying the input value X by the weight W and adding Bias is the formula for the result[37].

$$Y = f\left(\sum_{i=1}^N X_i W_{ki} + \theta_j\right)$$

$$\theta_j = j^{th} \text{ node bias}$$

$$f(\omega) = \text{activation function}$$

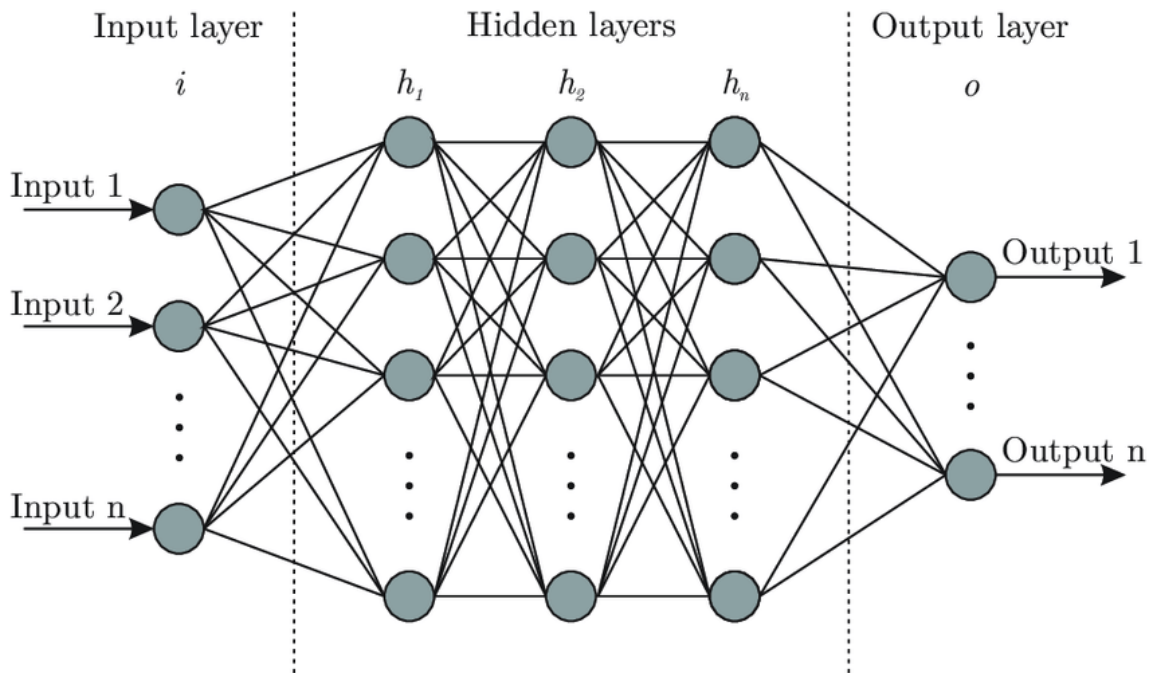


Figure 2.7 Structure of Artificial Neural Network(ANN)

As shown in the figure 2.5 above, the artificial neural network is divided into an input layer, a hidden layer, and an output layer. The input layer refers to a layer of neurons in which data is initially set, and the hidden layer is a layer of neurons that is literally hidden without data being revealed. The output layer is the neuron layer that contains the learned data we want to obtain. Neurons all have various combinations of weights and bias values, and control the weights and bias values during transmission.

However, if data is simply transferred from the input to the output, optimization of the data does not work well. If an error occurs in the target value, the weight is updated and the optimization is performed while the previous error is transmitted.[38].

2.4 Previous work

Since this study is an extension of the previous study, I will explain the previous study first. . The research topic was to develop a DED process for 10% cost reduction of double pipe manufacturing for ships. The double pipe is a passage through which LNG gas flows in the vessel, and is doubled to withstand the pressure, and is connected by a bridge between the pipes. The conventional manufacturing process is to manufacture two pipes and weld the inner bridge by welding. When the two pipes were connected by welding, a person had to work directly, and the space between the pipes was small, making it difficult to work. When it was manufactured using the DED process, it was possible to reduce the cost by uniting the existing complex production methods into one. In addition, in the DED method using an expensive metal powder, the optimization of process parameters was also conducted to reduce costs.

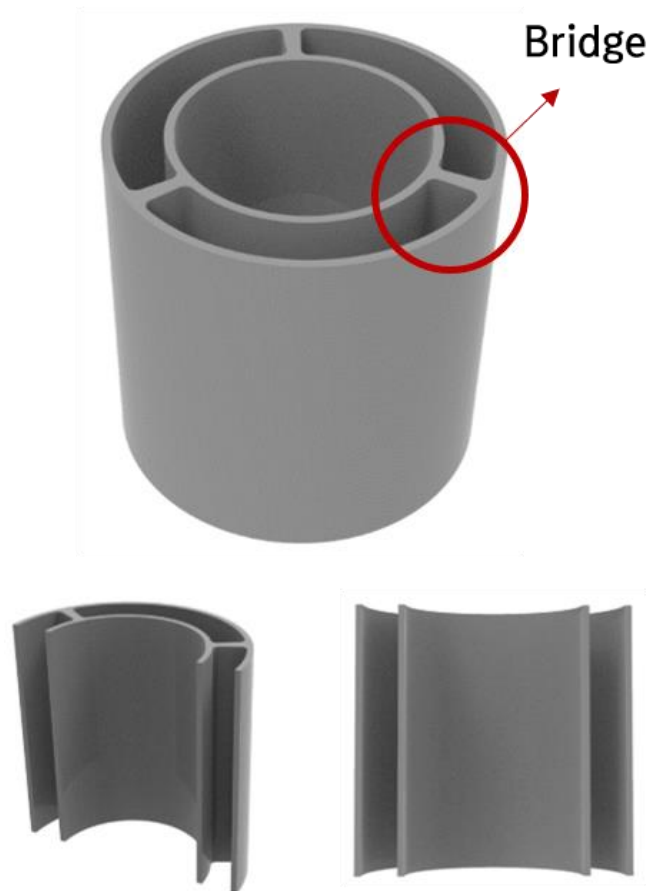


Figure 2.8 3D model of double pipe

Process parameter optimization

In order to achieve the objectives of the study, optimization studies of DED process parameters were conducted for SUS316L used for double pipe manufacturing. Laser power (LP), powder feed rate (PFR), and coaxial gas rate (CGR) were selected as key process parameters. Using the DOE technique, the variables were divided into a certain level to measure the results of single track, multi-track, and cube for each process variable. First, for the most important indicator, dimensional accuracy, the range of process variables was narrowed according to the dimensional quality of single track and multi-track, and 3d shapes were stacked to observe microstructure. Subsequently, various mechanical property tests were conducted to confirm the final selected process parameters.

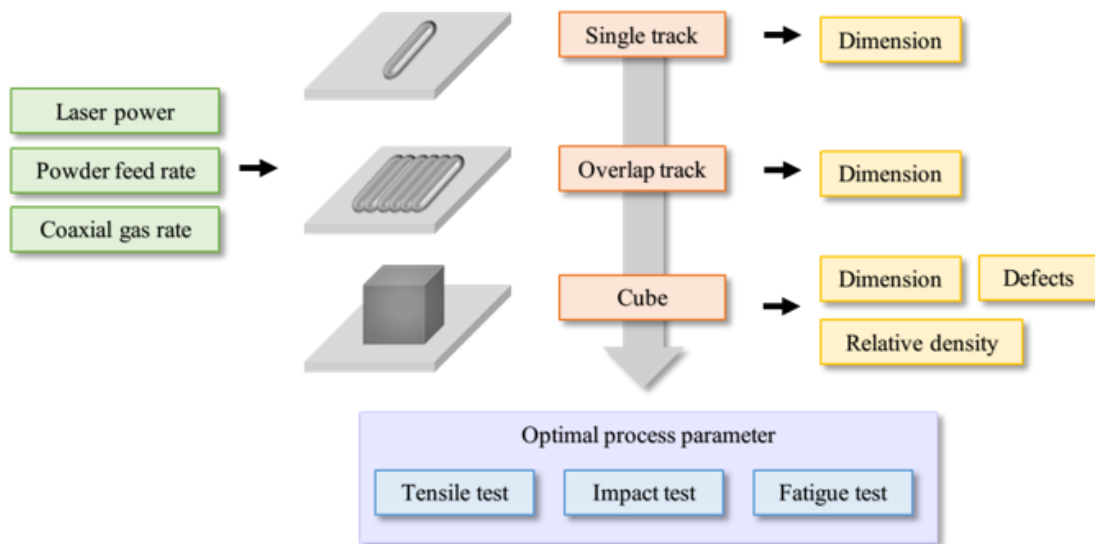


Figure 2.9 Experiment process of process parameter optimization

Single track

Three process parameter (LP, PFR, and CGR) were selected for each of the six levels with reference to the literature, resulting in a total of 216 data sets. Based on the generated data, a total of 216 single track samples were produced, and the cross section was photographed under a microscope to measure width and height.

Laser power [W]	Powder feed rate [g/min]	Coaxial gas rate [l/min]
350	3.5	4

450	4.5	5
550	5.5	6
650	6.5	7
750	7.5	8
850	8.5	9

Table 2.4 Value of process parameter

a.



b.



Figure 2.10 Actual deposited (a)dimension and (b)cross-section of single track

The target value of the dimensions of the single track was 0.8 to 1.0 mm in width and 0.17 mm in height. Since it is difficult to intuitively understand the correlation between process parameters and results, one process at a time method was used to compare the results with each process parameter. First, we confirmed the result of height and width for laser power that was intuitively easy to grasp. The laser power corresponding to the targeted dimension was confirmed to be 350W. Next, when the powder feed rate was 350~8.5 at 350W, the result was confirmed and satisfactory at 4.5 and 5.5. Lastly, in the case of coaxial gas, it was not possible to grasp the correlation with the result, so we consulted the equipment company and selected it as 7. Therefore, the primary process parameters were narrowed to 350 W, 4.5 to 5.5 g/min, 7 l/min.

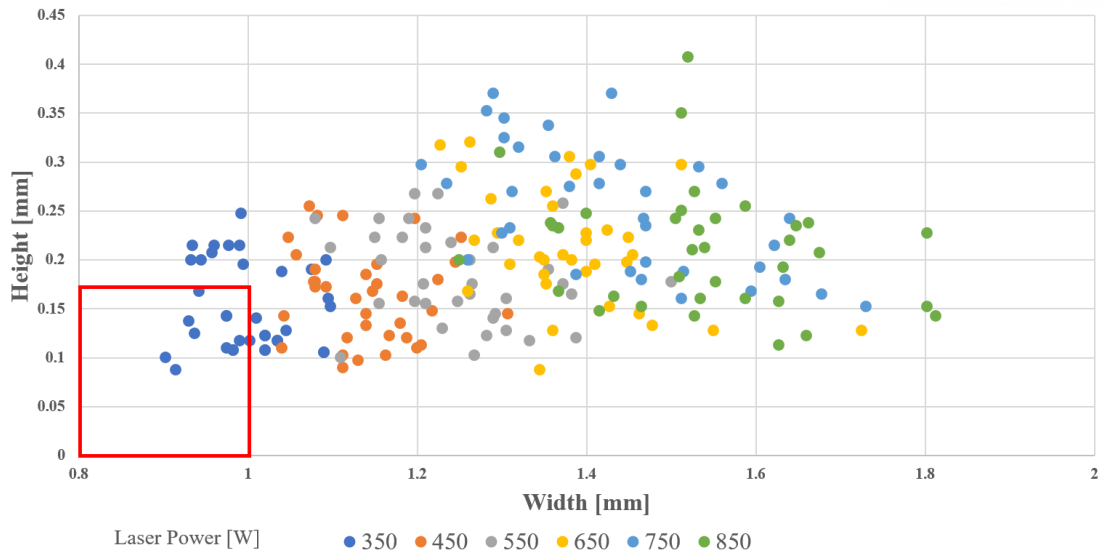


Figure 2.11 Width and Height of single track according to Laser power

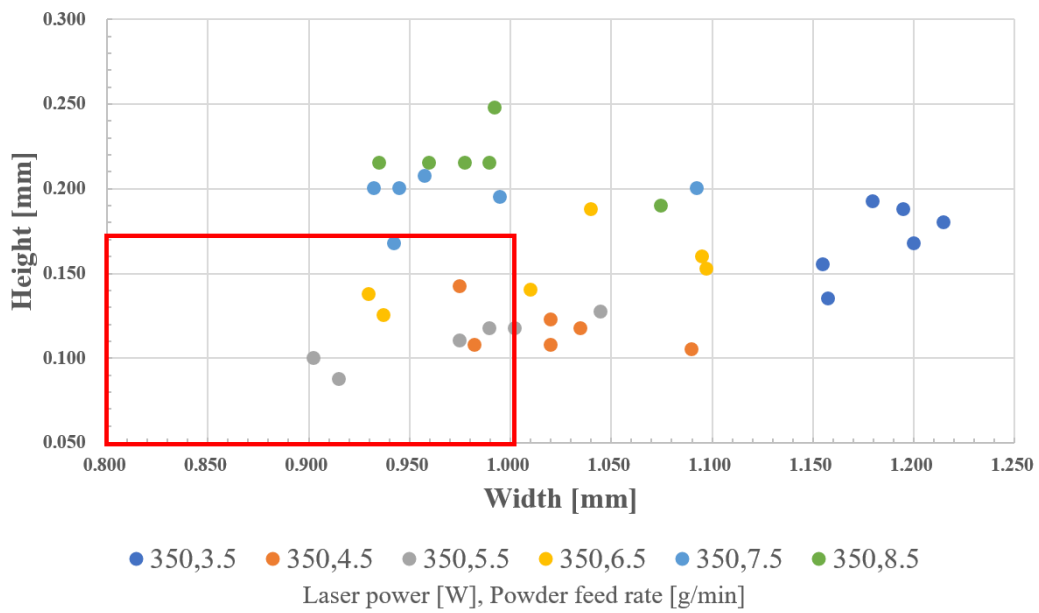


Figure 2.12 Width and Height of single track according to powder feed rate at 350W

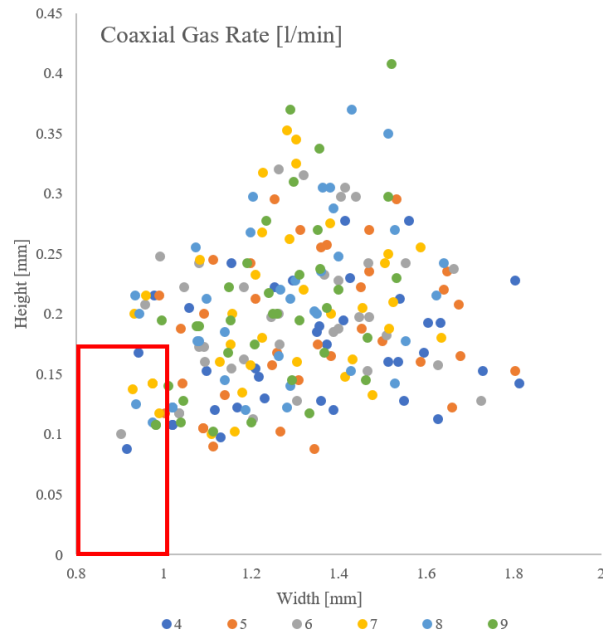


Figure 2.13 Width and Height of single track according to Coaxial gas rate

Laser power [W]	Powder feed rate [g/min]	Coaxial gas rate [l/min]
350	4.5, 5.5	7

Table 2.5 Optimal process parameter of single track

Multi-track

For more accurate results, the data set was created by resetting the powder feed rate of the 1st optimal process parameter at 0.1 intervals. In the case of multi-track, the target value was 0.25mm in height, and the powder feed rate satisfying this was selected as 4.5,4.8. Since the values of laser powder and coaxial gas rate were determined in a single track, the second optimal parameters were selected as 350W, 4.5,4.8g/min, and 7l/min.



Figure 2.14 Actual deposited multi-track

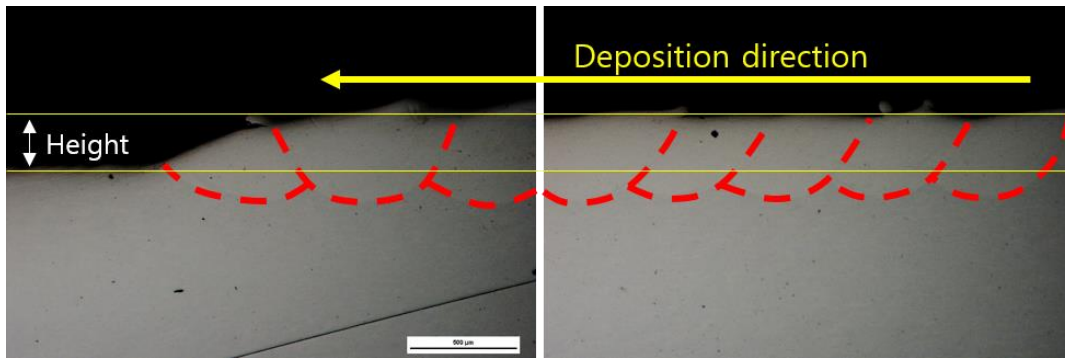


Figure 2.15 Cross section of multi-track

PFR [g/min]	Single [mm]		Multi [mm]	
	Width	Height	Width	Height
4.5	0.978	0.133	11.327	0.252
4.6	0.950	0.148	10.916	0.212
4.7	1.125	0.123	11.150	0.246
4.8	0.940	0.168	11.168	0.256
4.9	0.973	0.150	11.159	0.268
5.0	1.005	0.138	11.093	0.199
5.1	1.035	0.173	11.110	0.376
5.2	0.995	0.140	10.888	0.335
5.3	0.968	0.125	11.056	0.293
5.4	1.073	0.185	11.056	0.279
5.5	0.948	0.160	11.047	0.326

Table 2.6 Width and Height of Single and multi-track according to powder feed rate at 350W,7l/min

Cube

Cube specimens were made for a total of four data by adding 4.2 and 5.1 to the secondary optimal parameters, 4.5 and 4.8. The cube was made of 20*20*20 (mm) size, and relative density was added in addition to the dimensional precision as the target value. As shown in the Figure 2.14, in the 3D shape, the relative density was measured by observing the microstructure on the YZ and XZ cross section. As a result, 4.8 having the highest relative density was selected as the final powder feed rate, except 5.1, which did not satisfy the dimensions. Therefore, the final optimal parameters were determined to be 350 W, 4.8 g/min, 7 l/min.

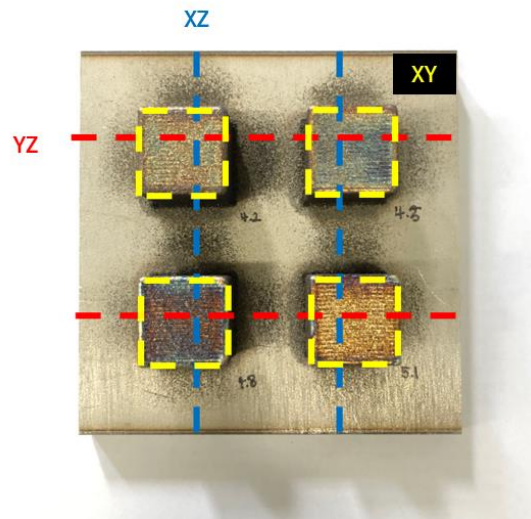


Figure 2.16 Actual deposited cube specimens

PFR[g/min]	4.2	4.5	4.8	5.1
Length [mm]	21.06	21.13	21.16	21.25
Width [mm]	21.11	21.13	21.23	21.29
Height [mm]	20.18	20.04	20.17	19.95

Table 2.7 Dimension of cube specimens according to powder feed rate

PFR [g/min]	Relative density			
	XY plane		YZ plane	
4.2	99.9554	Max. 99.978	99.974	Max. 99.979
		Min. 99.937		Min. 99.959
4.5	99.9296	Max. 99.962	99.9704	Max. 99.985
		Min. 99.902		Min. 99.954
4.8	99.9862	Max. 99.994	99.9872	Max. 99.995
		Min. 99.981		Min. 99.981
5.1	99.9902	Max. 99.997	99.977	Max. 99.985
		Min. 99.983		Min. 99.959

Table 2.8 Relative density of cube specimens according to powder feed rate

Laser power [W]	Powder feed rate [g/min]	Coaxial gas rate [l/min]
350	4.8	7

Table 2.9 Final Optimal process parameter

Mechanical Properties validation and printing

As a final process parameter, specimens were tested for mechanical properties verification. The test was conducted in a total of three tests: tensile test, impact test, and fatigue test. The test results were compared with test results of specimens produced by casting and rolling. The ultimate tensile strength of the specimen produced by the DED method was 577.04MPa, which was greater than the casting specimen strengths of 515 MPa. The result of the impact test was that the specimen produced by the DED method had an Absorption energy of 140J, which was higher than the 103J, Absorption energy of Castings.



Figure 2.17 (a)Tensile, (b)Impact, (c)Fatigue specimens of optimal parameter

	Condition	UTS(Mpa)	YS(Mpa)	Elongation(%)
Tensile test	4.8 g/min	577.04(±1.57)	413.54(±0.99)	50.31(±2.79)
	Castings	515	205	60

Table 2.10 Result of Tensile test and comparison to Castings

	Condition	Absorption energy (J)
Impact test	4.8 g/min	140.37(±0.93)
	Casting	103

Table 2.11 Result of Impact test and comparison to Castings

A total of 27 samples were prepared for the fatigue test, and the frequency was set to 27hz and

proceeded to 10^7 cycles. As a result, the fatigue limit was measured to be 300 MPa. According to ASTM A276, 35% of tensile strength based on 10^7 cycles is fatigue limit. Therefore, the fatigue limit of the specimen made of DED is higher than the fatigue limit of the existing manufacturing method, 175 MPa. As a result of the three tests, when manufactured in DED as the optimal process parameter, better mechanical properties than the existing products were derived in all tests, and finally, the prototype was completed. The powder required to make the prototype was 8 kg in total and the gas was 90l.

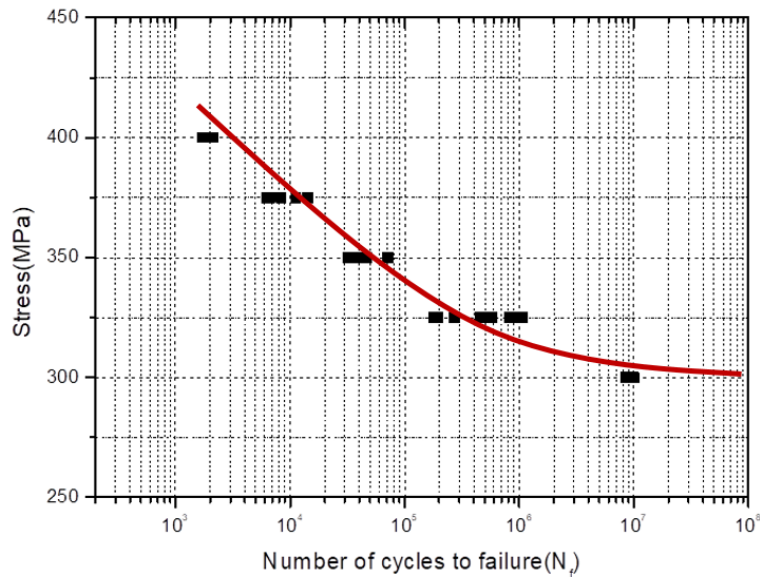


Figure 2.18 S-N curve of fatigue test

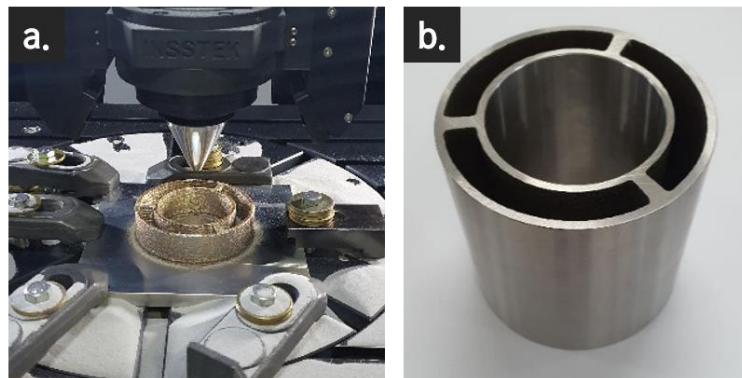


Figure 2.19 (a) Direct energy deposition of prototype and (b) final prototype

Limitation and motivation from previous work

In this study, there were many limitations in the method of setting process parameters. The first is the accuracy of the data. The analysis method called one factor at a time was used to understand the correlation with various quality according to the three key variables (LP, PFR, CGR). In this method, it is difficult to find the reliability of data because it is viewed in one-to-one in analyzing the relationship

between various data. For example, in the case of CGR, the relationship between the variable and the height and width of the single track was not found.

The other, I think, is inefficient in terms of time. In the previous study, appropriate process variables were selected through the dimensional quality of a single track. The laser power that satisfies the target was clearly classified as 350W, so it was possible to quickly identify the remaining process variables. However, more data will generally be needed because not all data can produce this result. Since data in most manufacturing fields takes a long time to collect, an efficient analysis method in terms of time will be required.

These problems can be solved by using a machine learning technique that can generate a predictive model using relatively little data and grasp the correlation between various data at once. These reasons motivated me to start this study.

3. Methodology

3.1 Experiment equipment and material used

Equipment

The equipment used in this study is the insstek MX-600 in Figure 3.1. The MX-600 is capable of 5-axis processing, can use various metal powders, and can spray up to three powders simultaneously. As an energy source, Co2 fiber laser can be used and output of up to 1kW is possible. Build size is 450*600*350(mm) and it is possible to deposit large area than other metal 3d printers. Therefore, it is mainly used for repairing of molds and aviation parts.



Figure 3.1 Insstek MX-600

Material

The metal powder used is SUS316L made in a spherical shape. The size of the particles is described as D10, D50, D90, which means less than 48 μm , 48-150 μm , 150 μm or more, respectively. The particle size of the powder used in the experiment was 3.1% D10, 94.9% D50 and 2% D90. The density of the powder is 4.61 g/cm^3 and the composition is shown in the Table 3.2 below.

D10	D50	D90
less than 48 μm (3.1%)	48-150 μm (94.9%)	150 μm or more(2%)

Table 3.1 Particle size of SUS316L powder

Element	Fe	Cr	Ni	Mo	Mn	Si	C	P
Content	Bal.	17.52	11.01	2.04	0.83	0.59	0.014	0.014

Table 3.2 Composition of SUS316L powder

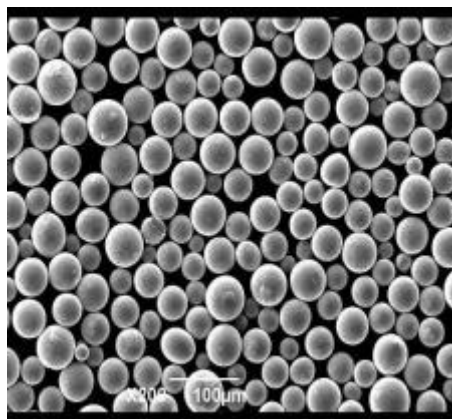


Figure 3.2 SEM image of SUS316L powder

3.2 Data selection

Input data

This study is to generate a predictive model by grasping the correlation between process variables and dimensional quality through machine learning. Therefore, the input data were selected as three process variables (Laser power, Powder feed rate, Coaxial gas) that have a great influence on the dimension. Due to the characteristics of the equipment, the range of input data is limited. Laser power is up to 1 kW , powder feed rate is up to 10 g/min , and coaxial gas rate is up to 10 l/min .

Input data	Range
Laser power [W]	0~1000

Powder feed rate [g/min]	0~10
Coaxial gas [l/min]	0~10

Table 3.2 Classification and range of Input data

Output data

In order to produce a 3d shape using DED, the 3D CAD file must be sliced in units of layers and converted into G-code. Magics for inststek was used as the conversion program.

Since the 3D shape is aggregations of layers, it was selected as the dimensional quality of the layer as out put data. Since the layer thickness of the equipment used in this study is set to a fixed value of 25 μ m, the target multi-track height was selected as 25 μ m. In addition, since the layer is aggregations of single tracks, the dimension of the single track was also selected as output data. Since the width of the single track is the beam diameter of the laser, which is the energy source, it was selected from 0.8 to 1.0mm. The height was selected to be 0.17 or less because the single track are stacked by hitting each other as much as hatching space and should be deposited to be 25 μ m layer thickness. Lastly, since the shape of the single track also affects the layer thickness, the angle was selected as the target dimension and the value was set to 15 degrees.

- Layer thickness : 0.25mm

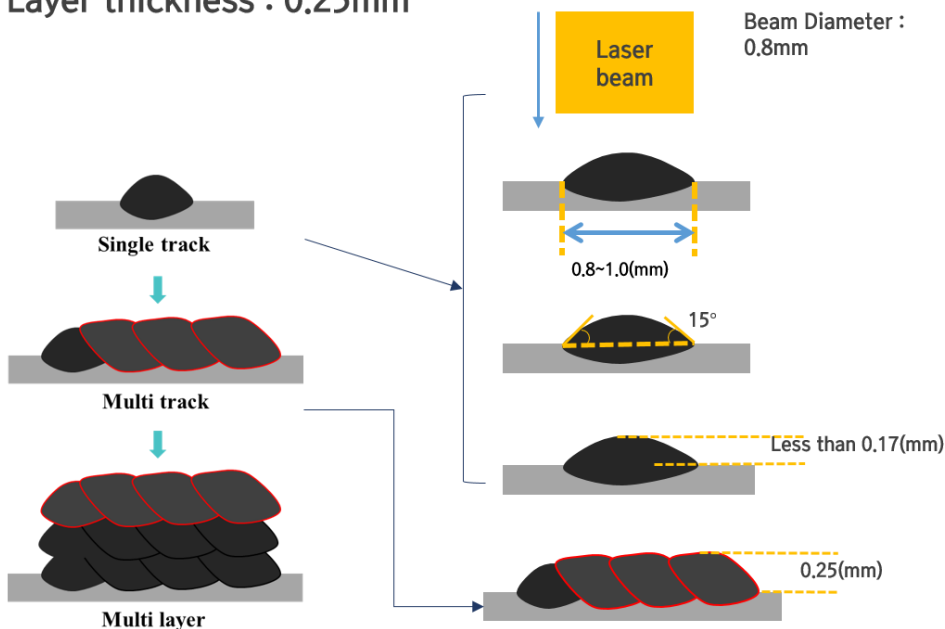


Figure 3.3 The schematic illustration of support vector regression

Target Dimension	
Height(single track)	Less than 0.17mm
Width(single track)	0.8~1.0mm
Angle Mean(single track)	15 degree
Height(Multi track)	0.25mm

Table 3.3 Target value of output data

3.3 Data collection and post-processing

As in the previous study, the three process parameters were divided into 6 levels, and a total of 216 input data sets were created to deposit single tracks and multi tracks. It was deposited on the same material SUS316L 150*150*10(mm) size substrate. The single track was printed in 10mm and the Multi-track was 10*10mm. After printing, it was cut with a wire cutting machine to pass through the center of the shape, and the cross section was photographed using a microscope to collect the output data set, which are Height(single track), Width(single track), Angle Mean(single track), and Height(Multi-track).

Laser power [W]	Powder feed rate [g/min]	Coaxial gas rate [l/min]
350	3.5	4
450	4.5	5
550	5.5	6
650	6.5	7
750	7.5	8
850	8.5	9

Table 3.4 Set of input data

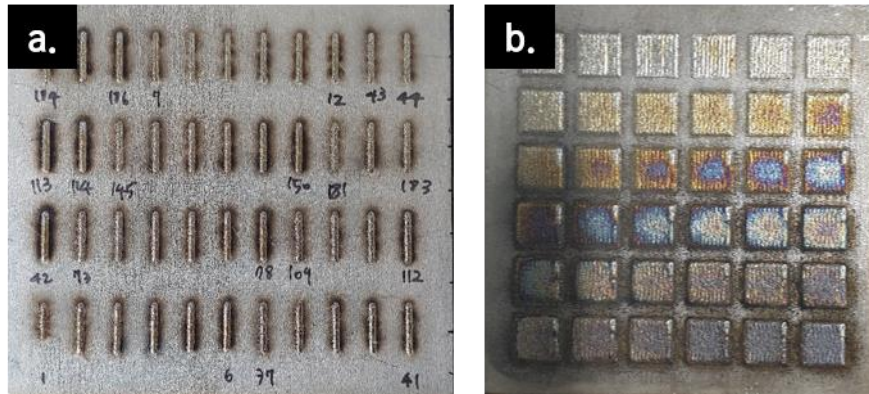


Figure 3.4 Deposition of (a)single track and (b)multi-track

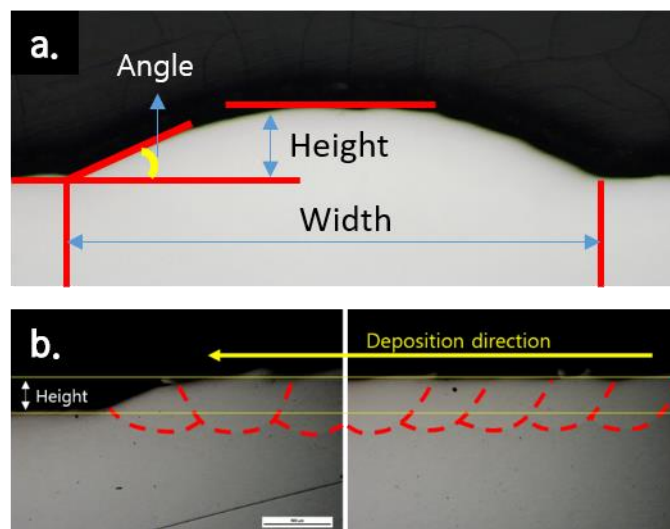


Figure 3.5 Cross section of (a)single track and (b)multi-track

Post processing of data

The following data are abbreviated, and LP, PFR, and CGR indicate laser power, powder feed rate, and coaxial gas rate, respectively, and are input data. The rest of the data is output data, and S and M next to the data name mean single track and multi-track, respectively.

Because the variance and average between the data are different, standardize the data using a standard scaler and randomize the data to increase the learning rate of the algorithm. And finally, in order to train and verify the model, the data was divided into 70% of training data and 30% of training data.

	LP	PFR	CGR	Width(S)	Height(S)	Angle_Mean	Height(M)
0	350	3.5	4	1.158	0.135	16.25	0.2216
1	350	3.5	5	1.155	0.155	14.80	0.2489
2	350	3.5	6	1.200	0.168	19.00	0.2598
3	350	3.5	7	1.215	0.180	19.20	0.2073
4	350	3.5	8	1.195	0.188	22.30	0.1928
...
211	850	8.5	5	1.648	0.235	17.95	0.9930
212	850	8.5	6	1.553	0.243	21.35	0.9580
213	850	8.5	7	1.513	0.250	23.00	0.8990
214	850	8.5	8	1.513	0.350	37.10	0.7960
215	850	8.5	9	1.520	0.408	41.70	0.7170

Table 3.5 Formation of data

	LP	PFR	CGR	Width(S)	Height(S)	Angle_Mean	Height(M)
14	-1.515537	-0.273097	-0.240411	-2.032093	-1.502572	-0.578354	-1.016727
138	0.267679	1.469339	-1.430643	0.635645	0.517252	-0.607707	1.627803
122	0.267679	-0.273097	-0.240411	0.753189	0.020064	0.825720	-0.486082
56	-0.921131	0.307715	-0.240411	-1.127515	-0.368363	0.346280	-0.242506
185	1.456490	-1.434722	1.544936	0.344340	-0.446049	-0.813182	-0.966708
...
203	1.456490	0.307715	1.544936	1.187590	0.517252	0.135914	0.340334
137	0.267679	0.888527	1.544936	0.267681	1.138736	0.840397	0.557812
72	-0.326726	-1.434722	-1.430643	0.446552	-1.191830	-0.504970	-0.931476
140	0.267679	1.469339	-0.240411	-0.192274	1.915592	0.497940	0.962321
37	-0.921131	-1.434722	-0.835527	-0.958865	-1.657943	-0.710444	-0.676157

Table 3.6 Normalized and randomly shuffled data

3.4 Generating predictive model

Goodness-of-fit test

The goodness-of-fit test is a statistical hypothesis that shows how well the generated prediction model fits the data, that is, how well it describes the data. There are various methods of these tests, but in this study, the Mean Absolute Error (MAE), Root Mean Squared Error (RMSE), R-square, and Mean

Absolute Percentage Error (MAPE), which are mainly used to verify the accuracy of the regression model, are used.

$$MAE = \frac{1}{n} \sum_{i=1}^n |y_i - \hat{y}|$$

$$MAPE = \frac{100}{n} \sum_{i=1}^n \left| \frac{y_i - \hat{y}}{y_i} \right|$$

$$RMSE = \frac{1}{n} \sum_{i=1}^n (y_i - \hat{y})^2$$

$$R^2 = 1 - \frac{SS_{RES}}{SS_{TOT}} = 1 - \frac{\sum (y_i - \hat{y})^2}{\sum (y_i - \bar{y})^2}$$

3.4.1 Predictive model of Multiple Linear Regression(MLR)

Multiple Linear Regression creates a single model through the Least square method without any parameters, so one result is derived. And the shape of the model is linear and it is a model for each output without considering the correlation between the target outputs.

MAE			
Width	Height	Angle mean	Height(M)
0.06596	0.02338	7.0393	0.06653
MAPE			
Width	Height	Angle mean	Height(M)
5.009	12.119	29.063	14.8044
RMSE			
Width	Height	Angle mean	Height(M)
0.08535	0.03202	9.0018	0.08565
R-squared			
Width	Height	Angle mean	Height(M)
0.8491	0.7028	0.4069	0.8512

Table 3.7 Model accuracy of MLR

3.4.2 Predictive model of Support Vector Regression(SVR)

Since the data type is non-linear, the RBF kernel was used, and the model was designed by changing the important values of C and γ . SVR is also a model that does not take into account correlation between outputs like MLR. Although it is difficult to fully explain the change of each result value by the

parameters of the SVR, the error was small when the C value was 2 rather than 1 and the error tended to decrease as the γ value increased. When all indicators are put together, the best model for the data is when C is 2 and γ is 0.2.

RBF Kernel		MAE				RMSE			
C	γ	Width	Height	Angle mean	Height (M)	Width	Height	Angle mean	Height (M)
1	0.01	0.07814	0.02302	7.3597	0.06561	0.09848	0.0328	9.745	0.09292
1	0.02	0.07194	0.02201	7.0937	0.05741	0.09216	0.03115	9.4779	0.0815
1	0.05	0.06749	0.02063	6.9709	0.0496	0.08675	0.0287	9.2624	0.07054
1	0.07	0.0675	0.02001	7.0257	0.0474	0.08671	0.02737	9.2531	0.06802
1	0.1	0.06791	0.01987	6.938	0.04475	0.08749	0.02652	9.0753	0.06623
1	0.2	0.06816	0.02008	6.7351	0.03868	0.08799	0.02625	8.7338	0.05815
1	0.3	0.06818	0.01989	6.7095	0.03745	0.08907	0.02625	8.7991	0.05409
2	0.01	0.07085	0.02257	7.0951	0.06107	0.09092	0.03172	9.4177	0.08583
2	0.02	0.06768	0.0216	6.9384	0.05279	0.08734	0.0304	9.2676	0.07526
2	0.05	0.06641	0.01965	7.0612	0.04713	0.08507	0.02702	9.2727	0.06749
2	0.07	0.06693	0.01953	6.9977	0.04516	0.08541	0.02621	9.1195	0.06536
2	0.1	0.06642	0.01963	6.8728	0.0411	0.0849	0.02583	8.8946	0.0617
2	0.2	0.06671	0.01949	6.6878	0.03684	0.08792	0.0249	8.7154	0.05513
2	0.3	0.06867	0.0197	6.5003	0.03686	0.09082	0.02539	8.6693	0.05088

RBF Kernel		R-squared				MAPE			
C	γ	Width	Height	Angle mean	Height (M)	Width	Height	Angle mean	Height (M)
1	0.01	0.7991	0.6881	0.3049	0.8249	6.0169	11.56	29.132	12.7191
1	0.02	0.8241	0.7187	0.3425	0.8653	5.4883	11.0516	27.706	11.3205
1	0.05	0.8441	0.7612	0.372	0.899	5.1397	10.0615	27.3519	9.8599
1	0.07	0.8442	0.78292	0.3733	0.9061	5.1243	9.7883	27.6451	9.467
1	0.1	0.8415	0.79607	0.3972	0.911	5.1332	9.8674	27.6365	8.9161
1	0.2	0.8396	0.8002	0.4417	0.9314	5.1655	10.345	26.8106	7.6277
1	0.3	0.8357	0.8002	0.4333	0.9406	5.1586	10.3233	26.4469	7.6067
2	0.01	0.8288	0.7083	0.3508	0.8506	5.3998	11.3996	28.0189	11.9977
2	0.02	0.842	0.7321	0.3713	0.8851	5.1404	10.803	27.2688	10.4039

2	0.05	0.85014	0.7883	0.3706	0.9076	5.0543	9.6503	27.8337	9.444
2	0.07	0.8489	0.8008	0.3913	0.9133	5.0858	9.7004	27.8862	9.0059
2	0.1	0.8507	0.80666	0.4209	0.9228	5.0457	9.9113	27.424	8.1173
2	0.2	0.8399	0.8203	0.44406	0.9383	5.0036	10.1618	26.4746	7.4063
2	0.3	0.8292	0.8131	0.4499	0.9475	5.1875	10.3426	25.5044	7.7532

Table 3.8 Model accuracy of SVR

3.4.3 Predictive model of Gradient Boosting Regression(GBR)

GBR, like SVR, is non-linear and does not consider the correlation between outputs. The optimal model was derived by adjusting the estimator representing the tree number of the model. The result shows that the error gradually decreases from 10 estimators, and then increases again from the moment it exceeds 50-60. The optimal model was selected when the number of trees was 60.

Estimator	MAE				RMSE			
	Width	Height	Angle mean	Height (M)	Width	Height	Angle mean	Height (M)
10	0.09957	0.02697	7.0856	0.09598	0.1236	0.03768	8.8946	0.1181
20	0.07862	0.02341	5.8938	0.06114	0.1004	0.03278	7.5496	0.0767
30	0.07381	0.02067	5.791	0.04541	0.09626	0.0292	7.4752	0.05684
50	0.07157	0.01985	5.6132	0.03061	0.09491	0.02673	7.2568	0.03932
60	0.07228	0.01982	5.5649	0.02786	0.09638	0.02658	7.1932	0.03619
80	0.07303	0.01956	5.6465	0.02507	0.09919	0.02604	7.1827	0.034
90	0.07368	0.01945	5.7247	0.02378	0.1006	0.02573	7.2753	0.03265
100	0.07457	0.01968	5.7937	0.02335	0.1018	0.02615	7.3377	0.03218
150	0.07995	0.0199	5.79391	0.02402	0.10784	0.02634	7.3981	0.03303
200	0.08247	0.0199	5.7014	0.02446	0.1099	0.02622	7.2978	0.03383
250	0.08563	0.02023	5.662	0.025	0.114	0.02654	7.2564	0.03503
300	0.08757	0.02048	5.8433	0.02658	0.1161	0.02668	7.42109	0.03664
400	0.09068	0.02077	6.0019	0.02794	0.1195	0.02712	7.5432	0.03755
500	0.09172	0.02102	6.0616	0.02907	0.1206	0.02744	7.6026	0.03873

Estimator	R-squared				MAPE			
	Width	Height	Angle	Height	Width	Height	Angle	Height
10	0.09957	0.02697	7.0856	0.09598	0.1236	0.03768	8.8946	0.1181
20	0.07862	0.02341	5.8938	0.06114	0.1004	0.03278	7.5496	0.0767
30	0.07381	0.02067	5.791	0.04541	0.09626	0.0292	7.4752	0.05684
50	0.07157	0.01985	5.6132	0.03061	0.09491	0.02673	7.2568	0.03932
60	0.07228	0.01982	5.5649	0.02786	0.09638	0.02658	7.1932	0.03619
80	0.07303	0.01956	5.6465	0.02507	0.09919	0.02604	7.1827	0.034
90	0.07368	0.01945	5.7247	0.02378	0.1006	0.02573	7.2753	0.03265
100	0.07457	0.01968	5.7937	0.02335	0.1018	0.02615	7.3377	0.03218
150	0.07995	0.0199	5.79391	0.02402	0.10784	0.02634	7.3981	0.03303
200	0.08247	0.0199	5.7014	0.02446	0.1099	0.02622	7.2978	0.03383
250	0.08563	0.02023	5.662	0.025	0.114	0.02654	7.2564	0.03503
300	0.08757	0.02048	5.8433	0.02658	0.1161	0.02668	7.42109	0.03664
400	0.09068	0.02077	6.0019	0.02794	0.1195	0.02712	7.5432	0.03755
500	0.09172	0.02102	6.0616	0.02907	0.1206	0.02744	7.6026	0.03873

			mean	(M)			mean	(M)
10	0.6836	0.5883	0.4209	0.7167	7.7976	14.5495	28.1337	22.664
20	0.7909	0.6886	0.5828	0.88073	6.0159	12.3714	23.5355	13.6804
30	0.80812	0.75282	0.591	0.93448	5.5986	10.8533	22.8449	9.8911
50	0.81348	0.7928	0.6145	0.9686	5.4197	10.4729	22.2395	6.6978
60	0.80764	0.7951	0.6212	0.9734	5.4494	10.4042	22.1641	6.1767
80	0.7962	0.8034	0.6224	0.9765	5.4647	10.2139	22.2982	5.7374
90	0.7904	0.808	0.6126	0.9783	5.4901	10.1487	22.466	5.4924
100	0.785	0.8017	0.6059	0.9789	5.5425	10.2269	22.7395	5.4331
150	0.7591	0.7988	0.5994	0.9778	5.9609	10.2453	22.9484	5.6738
200	0.7494	0.8006	0.6102	0.9767	6.1551	10.2375	23.0451	5.8531
250	0.73063	0.7958	0.6146	0.9751	6.4108	10.4107	23.0823	6.0133
300	0.7206	0.7936	0.5969	0.9727	6.5761	10.5399	24.1102	6.2915
400	0.7042	0.7867	0.5835	0.9714	6.8366	10.6557	25.1005	6.5124
500	0.6986	0.7817	0.5769	0.9695	6.9176	10.7794	25.3472	6.7378

Table 3.9 Model accuracy of GBR

3.4.4 Predictive model of Random Forest Regression(RFR)

The main parameter of the RFR is an estimator that shows the number of trees in the same way as GBR. However, RFR is a method of generating an optimal model when considering correlations among multiple outputs. Since the RFR randomly generates a tree and moves toward the target, the error is almost the same when the estimator is 30 or more. The most suitable parameter among them is when the estimator is 300.

Estimator	MAE				RMSE			
	Width	Height	Angle mean	Height (M)	Width	Height	Angle mean	Height (M)
10	0.08745	0.02335	5.5891	0.04703	0.1145	0.0294	7.5258	0.05936
20	0.09367	0.02062	5.534	0.04636	0.121	0.02791	7.4382	0.05743
30	0.08289	0.02132	5.1442	0.03832	0.115	0.02728	6.8777	0.04979
50	0.08759	0.02125	5.4112	0.03975	0.1167	0.02636	7.2367	0.05006
100	0.08362	0.02021	5.2308	0.03972	0.1094	0.02642	7.0837	0.05094
150	0.08666	0.01972	5.2984	0.04063	0.1124	0.02589	7.1662	0.05164
200	0.08648	0.02018	5.291	0.04249	0.113	0.02648	7.272	0.05315

250	0.08611	0.01952	5.0811	0.04043	0.11422	0.0258	6.9181	0.05204
300	0.08413	0.01954	5.0798	0.04154	0.1114	0.02553	6.8472	0.0525
400	0.08616	0.02009	5.1474	0.04044	0.1122	0.0258	6.9429	0.05175
500	0.08505	0.01994	5.1448	0.04054	0.1116	0.02621	7.0588	0.05138
600	0.08469	0.01976	5.1713	0.04124	0.1114	0.02599	7.0486	0.05276
700	0.08524	0.01989	5.2059	0.04027	0.1127	0.02578	7.0244	0.0507
800	0.08523	0.01989	5.1609	0.04082	0.1122	0.02613	7.0159	0.05196

Estimator	R-squared				MAPE			
	Width	Height	Angle mean	Height (M)	Width	Height	Angle mean	Height (M)
10	0.7282	0.7495	0.5854	0.9285	6.6803	12.6966	22.1262	10.5385
20	0.6966	0.7741	0.595	0.9331	7.2041	10.7439	21.5411	10.4072
30	0.7257	0.7843	0.6537	0.9497	6.2547	11.3031	21.1428	8.6847
50	0.7179	0.7985	0.6167	0.9491	6.6912	11.2858	21.9982	9.1533
100	0.7518	0.7976	0.6327	0.9473	6.3447	10.6361	21.1051	9.1389
150	0.7383	0.8057	0.6241	0.9459	6.5838	10.5165	21.3562	9.0794
200	0.7352	0.7967	0.6129	0.9427	6.5679	10.7165	21.3006	9.5798
250	0.7298	0.807	0.6497	0.945	6.5484	10.3733	20.4225	9.183
300	0.7428	0.811	0.6568	0.9441	6.3732	10.4164	20.6038	9.3452
400	0.7388	0.8071	0.6471	0.9457	6.5706	10.7422	20.7076	9.1593
500	0.742	0.8008	0.6353	0.9464	6.4635	10.5102	20.8038	9.0937
600	0.743	0.8042	0.6363	0.9435	6.4343	10.4268	20.8085	9.174
700	0.7369	0.8073	0.6388	0.9477	6.4734	10.5082	21.0292	9.1181
800	0.7392	0.802	0.6397	0.9452	6.4702	10.5538	20.8002	9.1947

Table 3.10 Model accuracy of RFR

3.4.5 Predictive model of Artificial Neural Network(ANN)

ANN is a non-linear model and updates the weights considering the correlation with the outputs. The most important parameters are the number of hidden layers and the number of nodes. Because of the small amount of data, the number of hidden layers was set to 2 and 3, and the number of nodes was gradually increased from 4 to 24 to create a model. As a result, the accuracy was highest when the number of hidden layers was 2 and the number of nodes was 24.

Hidden layer node	MAE				RMSE			
	Width	Height	Angle	Height	Width	Height	Angle	Height

			mean	(M)			mean	(M)
4--4	0.0827	0.02767	7.2784	0.07199	0.1114	0.03871	9.1967	0.08715
8--8	0.0641	0.02706	6.8654	0.06563	0.08401	0.0379	8.7345	0.08233
10--10	0.06662	0.02333	6.7019	0.04827	0.08479	0.03067	8.4517	0.06381
12--12	0.06562	0.02011	6.6244	0.04674	0.08547	0.02738	8.3811	0.06154
16--16	0.06418	0.02122	6.2677	0.04533	0.08485	0.02781	8.007	0.06138
20--20	0.06354	0.02044	6.3972	0.04191	0.08558	0.0268	8.0659	0.05715
24--24	0.06355	0.01976	6.1552	0.03184	0.08403	0.0252	7.8497	0.04076
4--4--4	0.0901	0.03233	7.0484	0.06845	0.1125	0.04154	9.0177	0.08074
8--8--8	0.07356	0.02308	6.6955	0.0465	0.09147	0.03144	8.4087	0.05972
10--10--10	0.06799	0.02399	6.289	0.06511	0.08827	0.03194	8.0967	0.08093
12--12--12	0.06739	0.02396	6.4442	0.04629	0.09027	0.03135	8.208	0.06093
16--16--16	0.06686	0.022	6.5151	0.04332	0.0875	0.02865	8.3897	0.05772
20--20--20	0.06712	0.02307	6.3981	0.03623	0.09418	0.02885	8.204	0.04543
24--24--24	0.06395	0.02207	6.129	0.04403	0.08525	0.02743	7.93133	0.05657

Hidden layer node	R-squared				MAPE			
	Width	Height	Angle mean	Height (M)	Width	Height	Angle mean	Height (M)
4--4	0.7425	0.5657	0.3809	0.846	6.0506	14.1589	30.9837	16.1824
8--8	0.8538	0.5835	0.44163	0.8625	4.8543	13.4591	28.1867	14.3407
10--10	0.8511	0.7272	0.4772	0.9174	5.0492	12.2681	27.5617	9.411
12--12	0.8487	0.7827	0.4858	0.9232	4.9451	10.3061	26.8972	9.7401
16--16	0.8509	0.7758	0.5307	0.9236	4.8077	11.2461	26.3519	8.7439
20--20	0.8483	0.7917	0.5238	0.9337	4.7705	10.8469	27.6148	8.5106
24--24	0.8537	0.8159	0.549	0.9663	4.8611	11.0795	26.8977	6.503
4--4--4	0.7375	0.4997	0.40483	0.8678	7.011	16.0303	28.7002	15.4592
8--8--8	0.8267	0.7134	0.4825	0.9276	5.6071	11.6734	27.3321	9.9769
10--10--10	0.8386	0.7042	0.5201	0.8671	5.1354	12.2463	26.6216	14.5711
12--12--12	0.8312	0.715	0.5069	0.9247	5.0686	12.482	26.7822	8.9912
16--16--16	0.8414	0.762	0.4848	0.9324	5.0699	11.725	27.9058	8.5565
20--20--20	0.8163	0.7587	0.5073	0.9581	5.078	12.5217	27.866	7.5703
24--24--24	0.8495	0.78188	0.5396	0.9351	4.8181	11.7526	25.576	9.2317

Table 3.11 Model accuracy of ANN

4. Result

Comparison of predictive models

		MLR	SVR	GBR	RFR	ANN
			C=2, $\gamma = 0.2$	Estimator = 60	Estimator = 300	Hidden layer node = 24--24
MAE	Width	0.06596	0.06671	0.07228	0.08413	0.06355
	Height	0.02338	0.01949	0.01982	0.01954	0.01976
	Angle mean	7.0393	6.6878	5.5649	5.0798	6.1552
	Height (M)	0.06653	0.03684	0.02786	0.04154	0.03184
RMSE	Width	0.08535	0.08792	0.09638	0.1114	0.08403
	Height	0.03202	0.0249	0.02658	0.02553	0.0252
	Angle mean	9.0018	8.7154	7.1932	6.8472	7.8497
	Height (M)	0.08565	0.05513	0.03619	0.0525	0.04076
R-squared	Width	0.8491	0.8399	0.80764	0.7428	0.8537
	Height	0.7028	0.8203	0.7951	0.811	0.8159
	Angle mean	0.4069	0.44406	0.6212	0.6568	0.549
	Height (M)	0.8512	0.9383	0.9734	0.9441	0.9663
MAPE	Width	5.009	5.0036	5.4494	6.3732	4.8611
	Height	12.119	10.1618	10.4042	10.4164	11.0795
	Angle mean	29.063	26.4746	22.1641	20.6038	26.8977
	Height (M)	14.8044	7.4063	6.1767	9.3452	6.503

Table 4.1 Comparison model accuracy

The optimal model was selected and compared among 5 regression models of MLR, SVR, GBR, RFR, and ANN. The values of MAE, RMSE, and MAPE indicate errors, so the lower is better, and the higher the R-square is, the better the prediction model because it is an indicator for evaluating the fit of the model. Although the results are not the best in all indicators, we can draw the conclusion that the model generated using the Artificial Neural Network (ANN) algorithm is better suited to explain the data in this study than other models.

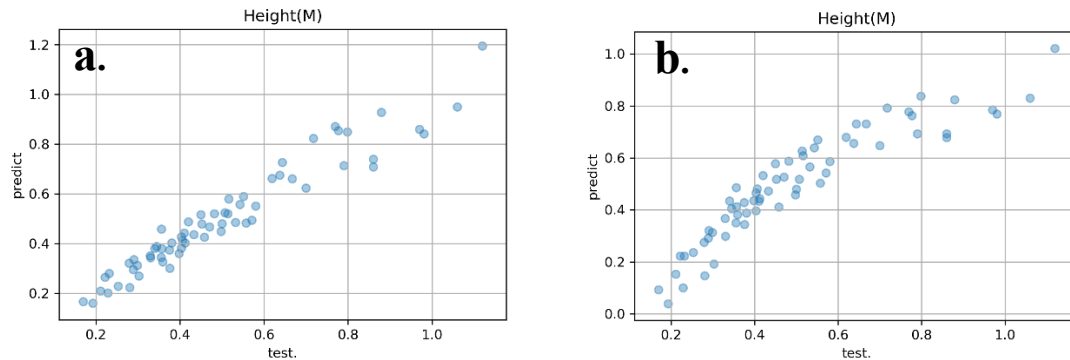


Figure 4.1 Scatter of multi-track height between actual and predicted value in (a)ANN and (b)MLR.

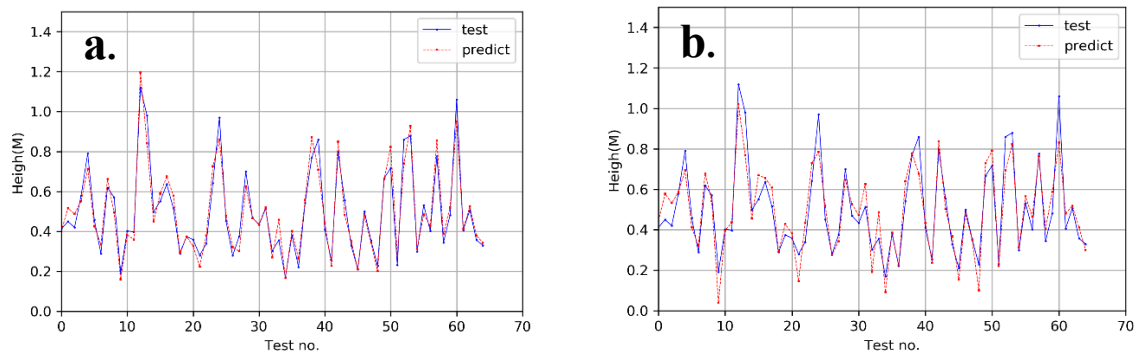


Figure 4.2 Plot of multi-track height value in (a)ANN and (b)MLR.

In particular, when predicting the height of the multi-track, a large difference occurred between MLR and ANN. As shown in figure 4.1 above, it can be seen that the ANN model is a straight line with the actual value and the predicted value almost identical, but in the MLR model it appears in the form of a curve. And in figure 4.2, you can see that in some samples in the MLR model, prediction is made with a large difference from the actual value.

Therefore, the optimal model was finally created using the ANN algorithm, and this model has 2 hidden layers and 24 nodes each. ReLU was used as the activation function and Adam was used as the optimizer. The model was trained with a total of 200 epochs and a batch of 20 sizes.

Artificial Neural Network(ANN)				
Activation	Optimizer	Hidden layer node	Epochs	Batch
ReLU	Adam	24-24	200	20

Performance(R-square)			
Width(S)	Height(S)	Height(M)	Angle
85.37%	81.59%	96.63%	54.9%

Table 4.2 Description of optimal predictive model

In the previous study, laser power, powder feed rate, and coaxial gas rate were derived as 350W, 4.8g/min, and 7l/min, respectively. At that time, the range of laser power was experimented at 350 to 850 at 100 intervals, but the result was that the dimension target of width was not satisfied above 350W. So, through the newly created prediction model, it was checked whether there are other optimal process parameters through range that were not used in the previous study.

Laser Power was set to 210~300 at intervals of 10, and the powder feed rate was set to 4.8 in the previous study, and it was set in 0.1 units from 0.1 to 4.8 with the goal of finding a parameter lower than this number. The coaxial gas rate was set from 1 to 9 in 1 unit. A total of 4320 new data were extracted and input to the prediction model, and 42 parameters satisfied target dimension, and among them, the variables closest to the target were predicted to be 300W, 3.7g/min, and 6l/min. It was lower in all values than the variables predicted by the existing method, especially in the case of powder feed rate, it was more than 1g. As mentioned in chapter 2. above, the amount of powder consumed when producing the prototype of the double tube was 8 kg. However, if it is manufactured through new process parameters, it can be produced by saving about 2kg of powder.

Laser power [W]	Powder feed rate [g/min]	Coaxial gas rate [l/min]
300	3.7	6

Table 4.3 Optimal process parameter from ANN predictive model

5. Conclusion and contribution

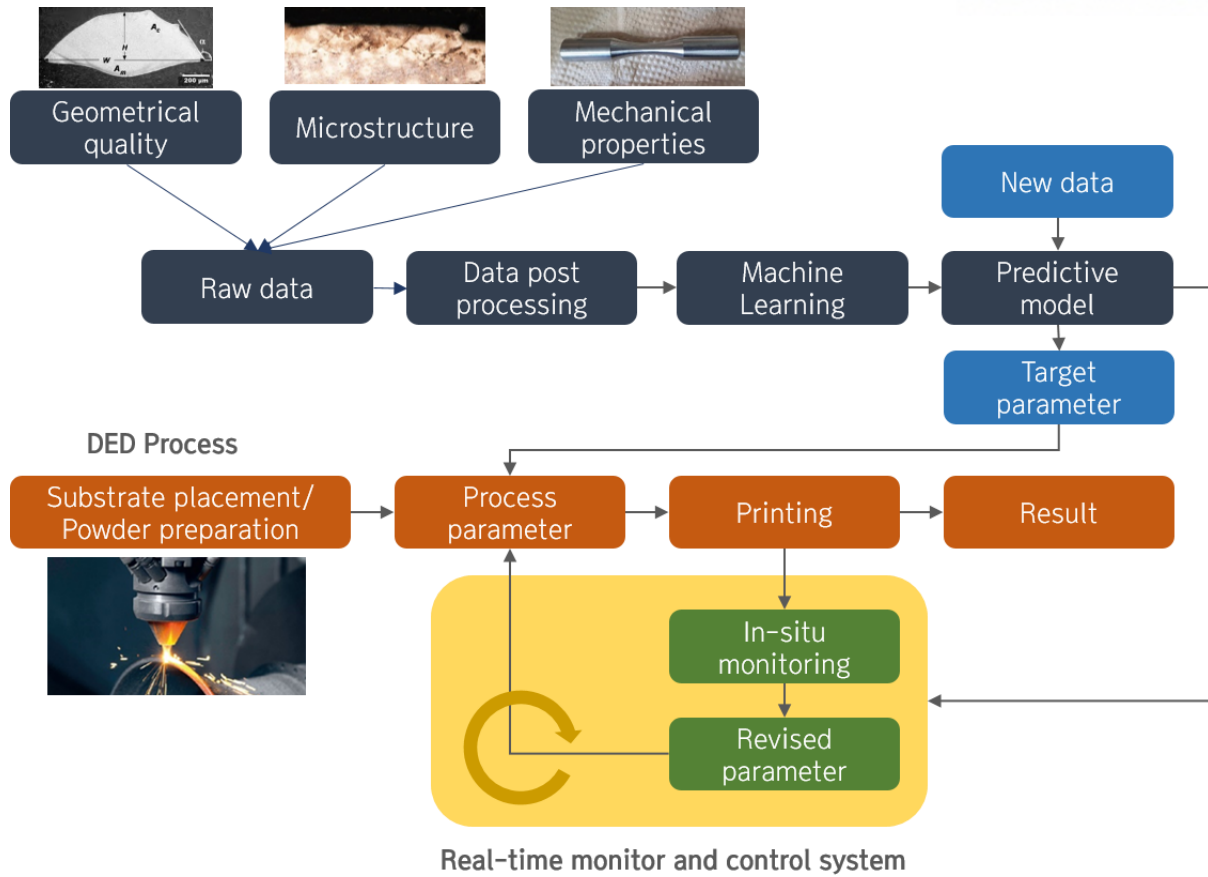
The one factor at a time analysis technique used in the previous process parameter optimization study is inaccurate and inefficient in time. To solve this problem, this study aims to create a model that predicts dimensional quality by applying machine learning to the DED process.

The 3D shape is aggregation of layers. Therefore, it can be said that the quality of a layer is important in manufacturing a product in additive manufacturing. To create a model that predicts the dimensional quality of a layer, three key process parameter (Laser Power, Powder Feed Rate, and Coaxial Gas) are set as input data, and the dimensional quality of single track and multi-track (Width, Height, Angle, Height(M)) as output data to perform the experiment. A total of 216 input data sets were created by setting the input data to 6 levels in total, and SUS316L powder was deposited on a substrate using an insstek MX-600 device to obtain output data for the data set.

In order to analyze the correlation between the data obtained through experiments, the data were pre-processed with a standard scaler and trained with five machine learning algorithms. As a result of training, the model trained with the ANN algorithm had the highest accuracy. When predicting the height of a multi-track, the accuracy was the highest with an R-square value of 96.63%. Optimal process parameter satisfying the target dimension were derived by inputting more than 4000 new datasets into this predictive model. The results are 300 W, 3.7 g/min, and 6 l/min for laser power, powder feed rate, and coaxial gas, respectively.

One factor at a time analysis technique was used or simple linear regression was used for optimizing process parameter so far. However, additive manufacturing technology is a complex process that has a number of process parameters to consider and those parameters have a great influence on product qualities. Therefore, the existing method of analyzing the correlation with one-to-one is not only significantly lower in accuracy, but also requires a large number of samples, which is inefficient in terms of time and cost.

In this complex process, training a model with data using machine learning techniques will be a great advantage in many ways. Although this study was a model development that predicts only dimensional quality, it is possible to develop a model that predicts microstructure or mechanical properties based on this study. Finally, these models are combined to complete an ideal process system that can monitor and control product quality in real time.



Real-time monitor and control system

Figure 5.1 Ideal DED process

Reference

- [1] Dilberoglu, U. M., Gharehpapagh, B., Yaman, U., & Dolen, M. (2017). The role of additive manufacturing in the era of industry 4.0. *Procedia Manufacturing*, 11, 545-554.
- [2] Herzog, D., Seyda, V., Wycisk, E., & Emmelmann, C. (2016). Additive manufacturing of metals. *Acta Materialia*, 117, 371-392.
- [3] Frazier, W. E. (2014). Metal additive manufacturing: a review. *Journal of Materials Engineering and Performance*, 23(6), 1917-1928.
- [4] Baumann, F. W., Sekulla, A., Hassler, M., Himpel, B., & Pfeil, M. (2018). Trends of machine learning in additive manufacturing. *International Journal of Rapid Manufacturing*, 7(4), 310-336.
- [5] Razvi, S. S., Feng, S., Narayanan, A., Lee, Y. T. T., & Witherell, P. (2019, August). A Review of Machine Learning Applications in Additive Manufacturing. In *ASME 2019 International Design Engineering Technical Conferences and Computers and Information in Engineering Conference*. American Society of Mechanical Engineers Digital Collection.
- [6] Qi, X., Chen, G., Li, Y., Cheng, X., & Li, C. (2019). Applying Neural-Network-Based Machine Learning to Additive Manufacturing: Current Applications, Challenges, and Future Perspectives. *Engineering*.
- [7] Baumgartl, H., Tomas, J., Buettner, R., & Merkel, M. (2020). A deep learning-based model for defect detection in laser-powder bed fusion using in-situ thermographic monitoring. *Progress in Additive Manufacturing*, 1-9. [8] The metallurgy and processing science of metal additive manufacturing
- [9] DebRoy, T., Wei, H. L., Zuback, J. S., Mukherjee, T., Elmer, J. W., Milewski, J. O., ... & Zhang, W. (2018). Additive manufacturing of metallic components—process, structure and properties. *Progress in Materials Science*, 92, 112-224.
- [10] Gong, H., Rafi, K., Gu, H., Starr, T., & Stucker, B. (2014). Analysis of defect generation in Ti–6Al–4V parts made using powder bed fusion additive manufacturing processes. *Additive Manufacturing*, 1, 87-98.
- [11] Bhavar, V., Kattire, P., Patil, V., Khot, S., Gujar, K., & Singh, R. (2014, September). A review on powder bed fusion technology of metal additive manufacturing. In *4th International conference and exhibition on Additive Manufacturing Technologies-AM-2014* (pp. 1-2).
- [12] Yadroitsev, I., Gusarov, A., Yadroitsava, I., & Smurov, I. (2010). Single track formation in selective laser melting of metal powders. *Journal of Materials Processing Technology*, 210(12), 1624-1631. [13] Effect of layer thickness setting on deposition characteristics in DED
- [14] Ghosh, S., & Choi, J. (2007). Deposition pattern based thermal stresses in single-layer laser aided direct material deposition process.
- [15] Xu, F., Madhavan, N., Dhokia, V., McAndrew, A. R., Colegrove, P. A., Williams, S., ... & Newman,

- S. T. (2016). Multi-sensor system for wire-fed additive manufacture of titanium alloy. In *26th International Conference on Flexible Automation and Intelligent Manufacturing, Seoul (North Korea)*.
- [16] Oh, W. J., Lee, W. J., Kim, M. S., Jeon, J. B., & Shim, D. S. (2019). Repairing additive-manufactured 316L stainless steel using direct energy deposition. *Optics & Laser Technology, 117*, 6-17.
- [17] Heigel, J. C., Michaleris, P., & Reutzel, E. W. (2015). Thermo-mechanical model development and validation of directed energy deposition additive manufacturing of Ti-6Al-4V. *Additive manufacturing, 5*, 9-19.
- [18] Shim, D. S., Baek, G. Y., & Lee, E. M. (2017). Effect of substrate preheating by induction heater on direct energy deposition of AISI M4 powder. *Materials Science and Engineering: A, 682*, 550-562.
- [19] Sciammarella, F. M., & Salehi Najafabadi, B. (2018). Processing Parameter DOE for 316L Using Directed Energy Deposition. *Journal of Manufacturing and Materials Processing, 2*(3), 61. (2)
- [20] 성선신, 종훈이, 성욱김, 준호황, & 현덕김. (2019). Effect of the Laser Beam Spot Size and Process Parameters on the Cross Section of SUS316L Parts using DED (Directed Energy Deposition). *Journal of Welding and Joining, 37*(5), 508-513.
- [21] Ugues, D., & Gennari, A. (2017). Influence of Directed Energy Deposition (DED) parameters on microstructural features of AISI 316L steel.
- [22] El Cheikh, H., Courant, B., Branchu, S., Hascoet, J. Y., & Guillén, R. (2012). Analysis and prediction of single laser tracks geometrical characteristics in coaxial laser cladding process. *Optics and Lasers in Engineering, 50*(3), 413-422.
- [23] Hansel, A., Mori, M., Fujishima, M., Oda, Y., Hyatt, G., Lavernia, E., & Delplanque, J. P. (2016). Study on consistently optimum deposition conditions of typical metal material using additive/subtractive hybrid machine tool. *Procedia CIRP, 46*, 579-582.
- [24] Yang, N., Yee, J., Zheng, B., Gaiser, K., Reynolds, T., Clemon, L., ... & Lavernia, E. J. (2017). Process-structure-property relationships for 316L stainless steel fabricated by additive manufacturing and its implication for component engineering. *Journal of Thermal Spray Technology, 26*(4), 610-626.
- [25] Oh, W. J., Son, Y., & Shim, D. S. (2019). Effect of In-Situ Post Heating on Repairing STS316L Built by Laser Powder Bed Fusion Using Direct Energy Deposition. *Korean Journal of Metals and Materials, 57*(8), 543-553.
- [26] Scime, L., & Beuth, J. (2018). Anomaly detection and classification in a laser powder bed additive manufacturing process using a trained computer vision algorithm. *Additive Manufacturing, 19*, 114-126.
- [27] Loh, W. Y. (2011). Classification and regression trees. *Wiley Interdisciplinary Reviews: Data Mining and Knowledge Discovery, 1*(1), 14-23.
- [28] Khanzadeh, M., Chowdhury, S., Tschopp, M. A., Doude, H. R., Marufuzzaman, M., & Bian, L. (2019). In-situ monitoring of melt pool images for porosity prediction in directed energy deposition

processes. *IISE Transactions*, 51(5), 437-455.

[29] Cheng, B., & Chou, K. (2013, August). Melt pool geometry simulations for powder-based electron beam additive manufacturing. In *24th Annual International Solid Freeform Fabrication Symposium-An Additive Manufacturing Conference, Austin, TX, USA* (pp. 644-654).

[30] Vapnik, V., *The nature of statistical learning theory*, Springer, 1996

[31] Lyu, J., & Manoochehri, S. (2019, August). Dimensional Prediction for FDM Machines Using Artificial Neural Network and Support Vector Regression. In *International Design Engineering Technical Conferences and Computers and Information in Engineering Conference* (Vol. 59179, p. V001T02A033). American Society of Mechanical Engineers.

[32] Lahiri, S. K., & Ghanta, K. C. (2008). The Support Vector Regression with the parameter tuning assisted by a differential evolution technique: Study of the critical velocity of a slurry flow in a pipeline. *Chemical Industry and Chemical Engineering Quarterly*, 14(3), 191-203.

[33] Shokri, S., Sadeghi, M. T., Marvast, M. A., & Narasimhan, S. (2015). Improvement of the prediction performance of a soft sensor model based on support vector regression for production of ultra-low sulfur diesel. *Petroleum Science*, 12(1), 177-188.

[34] Zhang, Y., & Haghani, A. (2015). A gradient boosting method to improve travel time prediction. *Transportation Research Part C: Emerging Technologies*, 58, 308-324.

[35] Natekin, A., & Knoll, A. (2013). Gradient boosting machines, a tutorial. *Frontiers in neurorobotics*, 7, 21.

[36] Saqib, S., Urbanic, R. J., & Aggarwal, K. (2014). Analysis of laser cladding bead morphology for developing additive manufacturing travel paths. *Procedia Cirp*, 17(0), 824-829.

[37] Baturynska, I., Semeniuta, O., & Martinsen, K. (2018). Optimization of process parameters for powder bed fusion additive manufacturing by combination of machine learning and finite element method: A conceptual framework.

[38] 순호권, 진우이, & 건희정. (2017). Snow damages estimation using artificial neural network and multiple regression analysis. *Journal of the Korean Society of Hazard Mitigation*, 17(2), 315-325.

Appendix A : MX-600 specification

Machine size	2000(W)×2900(L)×2550(H) mm
Machine weight	6,500kg
Laser type	Ytterbium Fiber laser
Laser Power	Max. 1kW
Gas	Argon(>99.999%)
X/Y/Z Stroke	450/600/380 mm
X/Y/Z Max. Traverse speed	200/200/150 mm/s
Tilt/Rotating Table(A/C)	-100~+5°/360°

Table A.1 Technical data

Appendix B : Fatigue test result in previous work

Stress [MPa]	400	400	400	375	375	375	375	375	350
Cycle [N]	1715	2100	2102	6255	6749	8310	11255	14312	31982
Stress [MPa]	350	350	350	350	325	325	325	325	325
Cycle [N]	35518	40637	46955	71554	180027	192692	272047	455880	496700
Stress [MPa]	325	325	325	325	300	300	300	300	300
Cycle [N]	576603	828896	1000000	1072200	1000000	1323491	8549370	10000000	10000000

Table B.1 Result of fatigue test

Appendix C : Dimensional quality data from all paramters

Laser Power [W]	Powder Feed Rate [g/min]	Coaxial Gas Rate [l/min]	Width of single track [mm]	Height of single track [mm]	Angle Mean value of single track [degree]	Height of multi-track [mm]
350	3.5	4	1.1575	0.135	16.25	0.2216
350	3.5	5	1.155	0.155	14.8	0.2489
350	3.5	6	1.2	0.1675	19	0.2598
350	3.5	7	1.215	0.18	19.2	0.2073
350	3.5	8	1.195	0.1875	22.3	0.1928
350	3.5	9	1.18	0.1925	26.7	0.1708
350	4.5	4	1.11	0.095	12.1	0.29
350	4.5	5	1.185	0.1025	11	0.238
350	4.5	6	1.1575	0.1225	16.1	0.162
350	4.5	7	1.025	0.1125	15.2	0.11
350	4.5	8	1.105	0.1125	15.45	0.189
350	4.5	9	1.0925	0.095	11.35	0.17
350	5.5	4	0.915	0.0875	12.9	0.374
350	5.5	5	1.0025	0.1175	13.9	0.323
350	5.5	6	0.9025	0.1	21.05	0.278
350	5.5	7	0.99	0.1175	23.35	0.256
350	5.5	8	0.975	0.11	20.75	0.253
350	5.5	9	1.045	0.1275	22.05	0.258
350	6.5	4	1.0975	0.1525	23.7	0.452
350	6.5	5	1.04	0.1875	26.2	0.433
350	6.5	6	1.095	0.16	38.05	0.353
350	6.5	7	0.93	0.1375	29.1	0.344
350	6.5	8	0.9375	0.125	25.6	0.289
350	6.5	9	1.01	0.14	23.4	0.235
350	7.5	4	0.9425	0.1675	28.75	0.7
350	7.5	5	1.0925	0.2	23.55	0.58
350	7.5	6	0.9575	0.2075	36.35	0.56
350	7.5	7	0.9325	0.2	28.05	0.5
350	7.5	8	0.945	0.2	27.8	0.41
350	7.5	9	0.995	0.195	29.15	0.38
350	8.5	4	0.9775	0.215	53.4	0.621
350	8.5	5	0.99	0.215	43.08	0.551
350	8.5	6	0.9925	0.2475	50.6	0.479
350	8.5	7	0.96	0.215	45.05	0.45
350	8.5	8	0.935	0.215	43	0.42
350	8.5	9	1.075	0.19	40.75	0.356
450	3.5	4	1.12	0.135	20.65	0.3998
450	3.5	5	1.185	0.1675	19.7	0.3563
450	3.5	6	1.2225	0.22	21.45	0.3028
450	3.5	7	1.1875	0.1725	19.35	0.2802
450	3.5	8	1.0975	0.1725	21	0.2283

450	3.5	9	1.2475	0.185	28.3	0.1931
450	4.5	4	0.95	0.0975	11.5	0.362
450	4.5	5	0.91	0.12	16.2	0.34
450	4.5	6	1.305	0.1525	18.45	0.289
450	4.5	7	1.345	0.1575	17.4	0.272
450	4.5	8	1.1675	0.1375	21.25	0.263
450	4.5	9	1.3875	0.145	13.4	0.211
450	5.5	4	1.1175	0.12	25.5	0.454
450	5.5	5	1.3075	0.145	25.4	0.403
450	5.5	6	1.1825	0.1625	26.05	0.375
450	5.5	7	1.1275	0.16	25.95	0.376
450	5.5	8	1.14	0.185	23.05	0.347
450	5.5	9	1.2	0.11	19.85	0.32
450	6.5	4	1.2175	0.1475	17.8	0.503
450	6.5	5	1.0425	0.1425	31.7	0.485
450	6.5	6	1.08	0.1725	30.5	0.456
450	6.5	7	1.1525	0.175	32.05	0.421
450	6.5	8	1.0775	0.1775	51.35	0.403
450	6.5	9	1.1475	0.1675	29.4	0.355
450	7.5	4	1.0575	0.205	22.75	0.64
450	7.5	5	1.1975	0.2425	22.85	0.64
450	7.5	6	1.245	0.1975	23.05	0.58
450	7.5	7	1.225	0.18	23.75	0.52
450	7.5	8	1.08	0.1775	38.8	0.47
450	7.5	9	1.08	0.19	57.9	0.45
450	8.5	4	1.2525	0.2225	27.25	0.796
450	8.5	5	1.1125	0.245	28.15	0.667
450	8.5	6	1.0475	0.2225	27.1	0.659
450	8.5	7	1.0825	0.245	31.6	0.543
450	8.5	8	1.0725	0.255	24.95	0.483
450	8.5	9	1.1525	0.195	18.6	0.435
550	3.5	4	1.1925	0.1525	21.8	0.2976
550	3.5	5	1.4725	0.175	15.05	0.3301
550	3.5	6	1.205	0.1825	20.7	0.2908
550	3.5	7	1.085	0.175	27.6	0.2792
550	3.5	8	1.165	0.1625	19.95	0.2196
550	3.5	9	1.185	0.1875	21.65	0.2158
550	4.5	4	1.26	0.0875	12.55	0.412
550	4.5	5	1.4425	0.11	15.2	0.374
550	4.5	6	1.24	0.135	19.45	0.365
550	4.5	7	1.1575	0.1275	19.75	0.304
550	4.5	8	1.245	0.1175	17.7	0.284
550	4.5	9	1.29	0.1175	14.2	0.26
550	5.5	4	1.21	0.155	26.75	0.571
550	5.5	5	1.2475	0.1575	30.25	0.453
550	5.5	6	1.265	0.175	25.1	0.396
550	5.5	7	1.1975	0.1575	32.5	0.429
550	5.5	8	1.2625	0.165	30.75	0.352
550	5.5	9	1.2075	0.175	27.2	0.299
550	6.5	4	1.3725	0.175	26.65	0.659

550	6.5	5	1.5	0.1775	27.4	0.599
550	6.5	6	1.2625	0.2	34.75	0.575
550	6.5	7	1.1575	0.2	43.35	0.557
550	6.5	8	1.29	0.2125	30.95	0.498
550	6.5	9	1.24	0.2175	35.5	0.458
550	7.5	4	1.355	0.19	27.2	0.79
550	7.5	5	1.21	0.2125	45.4	0.79
550	7.5	6	1.1825	0.2225	38.75	0.7
550	7.5	7	1.21	0.2325	58.35	0.64
550	7.5	8	1.0975	0.2125	48.55	0.64
550	7.5	9	1.15	0.2225	45.8	0.55
550	8.5	4	1.155	0.2425	22.75	0.798
550	8.5	5	1.3725	0.2575	21.9	0.73
550	8.5	6	1.08	0.2425	33.1	0.658
550	8.5	7	1.225	0.2675	22.75	0.608
550	8.5	8	1.1975	0.2675	23.1	0.547
550	8.5	9	1.19	0.2425	25.3	0.516
650	3.5	4	1.2775	0.1325	14.9	0.3445
650	3.5	5	1.155	0.155	23.95	0.353
650	3.5	6	1.125	0.1725	29.6	0.2849
650	3.5	7	1.125	0.1675	22.75	0.2686
650	3.5	8	1.36	0.16	16.75	0.2316
650	3.5	9	1.19	0.155	19.65	0.2143
650	4.5	4	1.1375	0.105	14.45	0.46
650	4.5	5	1.405	0.1225	22.3	0.384
650	4.5	6	1.3625	0.14	13.6	0.357
650	4.5	7	1.32	0.1375	16.85	0.329
650	4.5	8	1.26	0.1125	10.6	0.29
650	4.5	9	1.26	0.1425	16.75	0.279
650	5.5	4	1.41	0.195	29.2	0.548
650	5.5	5	1.26	0.1675	46.6	0.477
650	5.5	6	1.4475	0.1975	35.4	0.4
650	5.5	7	1.455	0.205	22.9	0.403
650	5.5	8	1.35	0.2	29.1	0.377
650	5.5	9	1.3725	0.205	27.95	0.342
650	6.5	4	1.35	0.185	33.05	0.712
650	6.5	5	1.45	0.2225	44.15	0.637
650	6.5	6	1.4	0.2275	31.8	0.577
650	6.5	7	1.32	0.22	36.75	0.523
650	6.5	8	1.2675	0.22	36.65	0.507
650	6.5	9	1.4	0.22	31.85	0.496
650	7.5	4	1.295	0.2275	38.7	0.86
650	7.5	5	1.36	0.255	31.45	0.91
650	7.5	6	1.405	0.2975	50.95	0.86
650	7.5	7	1.2875	0.2625	41.3	0.71
650	7.5	8	1.3875	0.2875	39.55	0.65
650	7.5	9	1.3525	0.27	35.55	0.64
650	8.5	4	1.425	0.23	20.75	0.886
650	8.5	5	1.2525	0.295	27.1	0.803
650	8.5	6	1.2625	0.32	32.05	0.733

650	8.5	7	1.2275	0.3175	40.2	0.712
650	8.5	8	1.38	0.305	30.15	0.632
650	8.5	9	1.5125	0.2975	31.45	0.58
750	3.5	4	1.205	0.12	13.25	0.4535
750	3.5	5	1.2	0.1625	17.1	0.3756
750	3.5	6	1.0525	0.175	27.8	0.3594
750	3.5	7	1.045	0.1625	19.15	0.3179
750	3.5	8	1.18	0.1475	19.4	0.3062
750	3.5	9	1.185	0.1875	26.2	0.2935
750	4.5	4	1.1975	0.0875	12.1	0.532
750	4.5	5	1.345	0.115	16.75	0.466
750	4.5	6	1.2175	0.13	14	0.429
750	4.5	7	1.2025	0.145	22.7	0.375
750	4.5	8	1.1075	0.1025	17.05	0.359
750	4.5	9	1.0675	0.09	12.75	0.329
750	5.5	4	1.605	0.1925	27.1	0.665
750	5.5	5	1.47	0.235	40.45	0.575
750	5.5	6	1.4675	0.2425	39.55	0.55
750	5.5	7	1.38	0.275	41.15	0.47
750	5.5	8	1.64	0.2425	24.55	0.406
750	5.5	9	1.31	0.2325	42.75	0.34
750	6.5	4	1.595	0.1675	19.5	0.777
750	6.5	5	1.3125	0.27	25.65	0.726
750	6.5	6	1.44	0.2975	31.25	0.657
750	6.5	7	1.3025	0.325	37.25	0.61
750	6.5	8	1.205	0.2975	25.25	0.555
750	6.5	9	1.235	0.2775	28.35	0.519
750	7.5	4	1.415	0.2775	39.8	1.14
750	7.5	5	1.5325	0.295	41.75	1.09
750	7.5	6	1.415	0.305	54.1	0.98
750	7.5	7	1.2825	0.3525	59.95	1
750	7.5	8	1.3625	0.305	55.9	0.86
750	7.5	9	1.355	0.3375	49.1	0.7
750	8.5	4	1.56	0.2775	27.1	1.117
750	8.5	5	1.47	0.27	25.3	0.98
750	8.5	6	1.32	0.315	30.45	0.869
750	8.5	7	1.3025	0.345	31.9	0.754
750	8.5	8	1.43	0.37	39.05	0.707
750	8.5	9	1.29	0.37	34.9	0.643
850	3.5	4	1.29	0.1575	15.3	0.4532
850	3.5	5	1.07	0.1325	15.05	0.4207
850	3.5	6	1.3675	0.1475	13.6	0.3976
850	3.5	7	1.1425	0.1675	16.4	0.3785
850	3.5	8	1.1275	0.1475	22.2	0.3531
850	3.5	9	1.18	0.14	18.65	0.2895
850	4.5	4	1.2525	0.1225	19.1	0.514
850	4.5	5	1.3725	0.1425	12.75	0.428
850	4.5	6	1.32	0.13	16.9	0.414
850	4.5	7	1.315	0.1275	16.8	0.394
850	4.5	8	1.2375	0.1325	16.15	0.363

850	4.5	9	1.305	0.1325	15.05	0.332
850	5.5	4	1.535	0.16	16.85	0.594
850	5.5	5	1.5875	0.16	28.35	0.619
850	5.5	6	1.51	0.1825	42.7	0.526
850	5.5	7	1.525	0.21	34.3	0.482
850	5.5	8	1.36	0.235	33.3	0.4
850	5.5	9	1.3575	0.2375	32.1	0.367
850	6.5	4	1.8025	0.2275	14.3	0.879
850	6.5	5	1.675	0.2075	13.7	0.769
850	6.5	6	1.6625	0.2375	19.7	0.746
850	6.5	7	1.505	0.2425	18	0.671
850	6.5	8	1.5275	0.27	29.3	0.647
850	6.5	9	1.5325	0.23	28.35	0.59
850	7.5	4	1.6325	0.1925	23.45	1.21
850	7.5	5	1.64	0.22	39.45	1.08
850	7.5	6	1.3675	0.2325	30.8	1.06
850	7.5	7	1.5875	0.255	28.1	0.97
850	7.5	8	1.4	0.2475	35.4	0.95
850	7.5	9	1.2975	0.31	49.7	0.86
850	8.5	4	1.54	0.2125	20.95	1.119
850	8.5	5	1.6475	0.235	17.95	0.993
850	8.5	6	1.5525	0.2425	21.35	0.958
850	8.5	7	1.5125	0.25	23	0.899
850	8.5	8	1.5125	0.35	37.1	0.796
850	8.5	9	1.52	0.4075	41.7	0.717

Table C.1 Full data set

Appendix D : Python code of Algorithms

```
# Multiple Linear Regression(MLR)
model = LinearRegression()

# Support Vector Regression(SVR)
model = MultiOutputRegressor(SVR(kernel='rbf',
                                  gamma=0.3,
                                  C=2.0))

# Gradient Boosting Regression(GBR)
params = {'n_estimators': 500,
          'learning_rate': 0.1,
          'loss': 'ls'}
reg = MultiOutputRegressor(ensemble.GradientBoostingRegressor(**params))

# Random Forest Regression(RFR)
reg = RandomForestRegressor(n_estimators = 800)

# Artificial Neural Network(ANN)
model = Sequential()
model.add(Dense(24, input_dim=3, kernel_initializer='normal', activation='relu'))
model.add(Dense(24, activation='relu'))
model.add(Dense(4, activation='linear'))
model.summary()
model.compile(loss='mse', optimizer='Adam', metrics=['mse', 'mae'])
>>> history = model.fit(X_train, y_train, epochs=200, batch_size=20, verbose=1, validation_split=0.2)
```

Figure D.1 Python Code of all algorithms used

Appendix E : Model comparison(ANN vs MLR) using scatter and plot

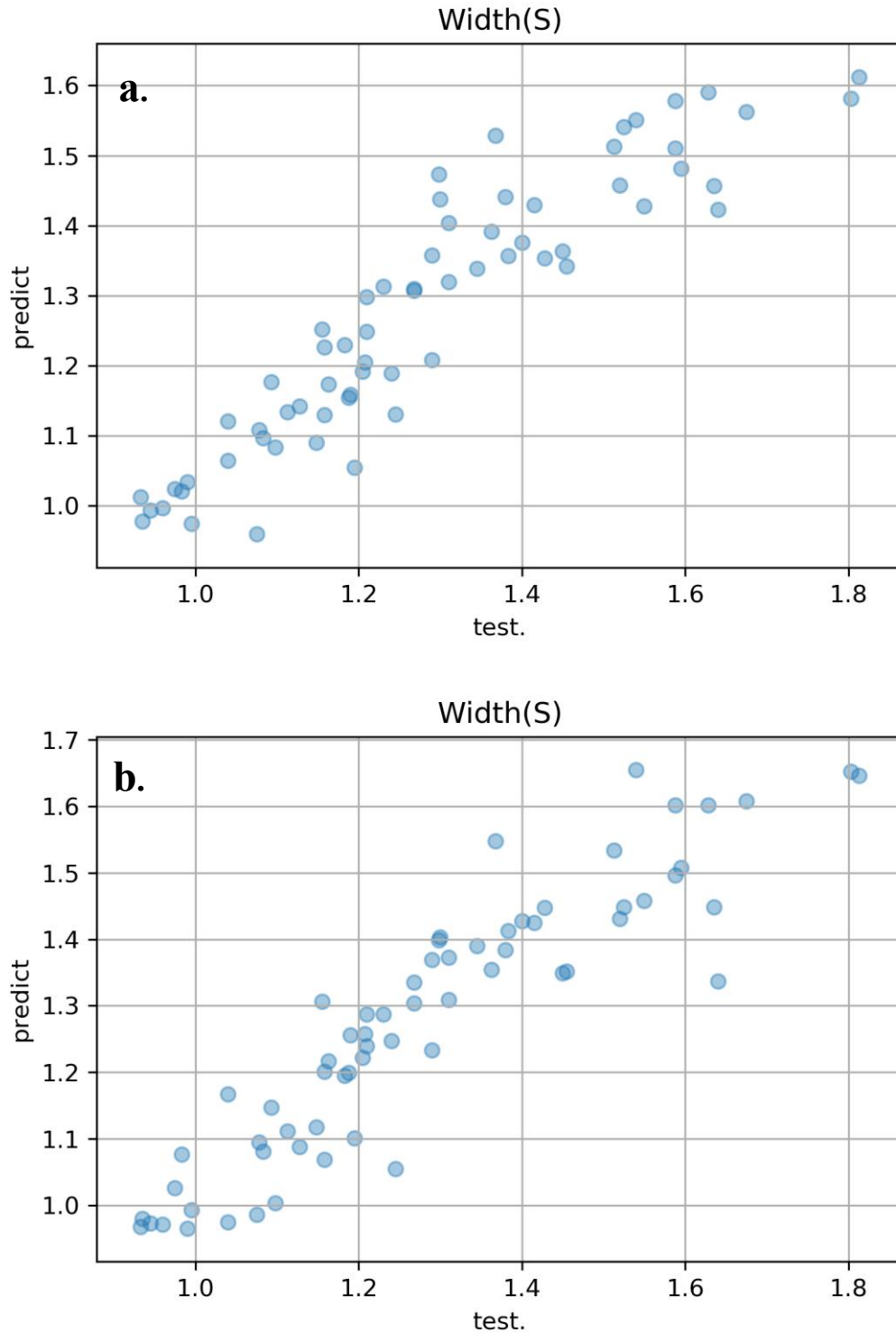


Figure E.1 Scatter of single track width between actual and predicted value in (a)ANN and (b)MLR.

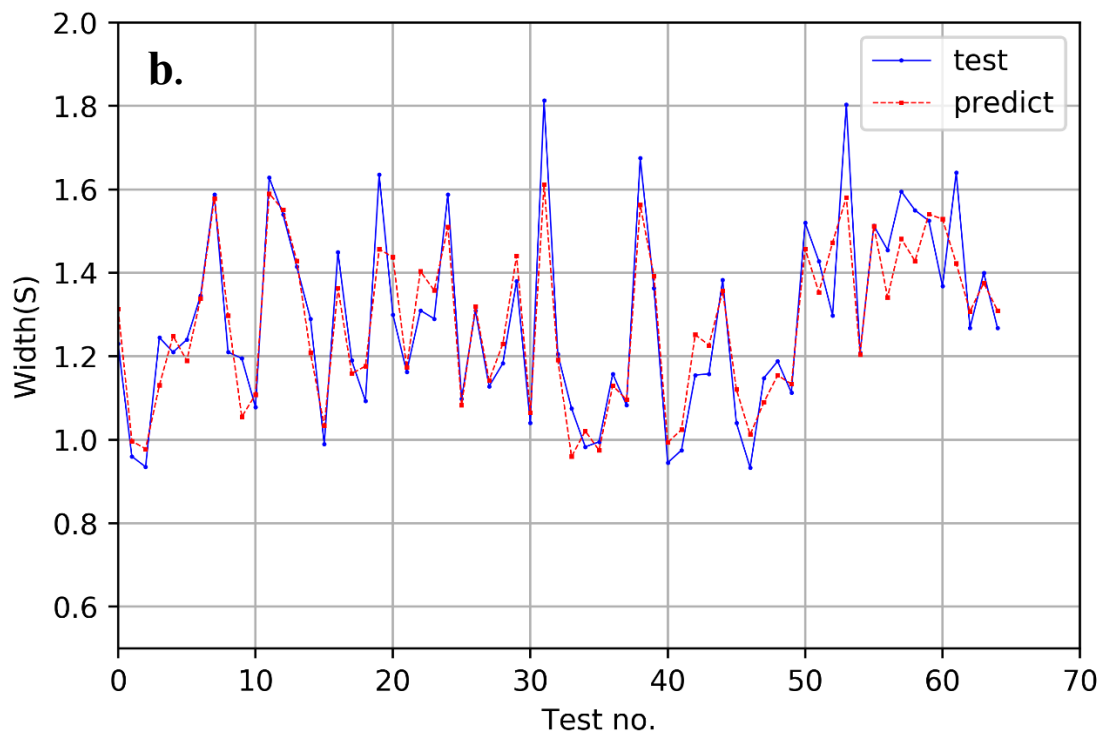
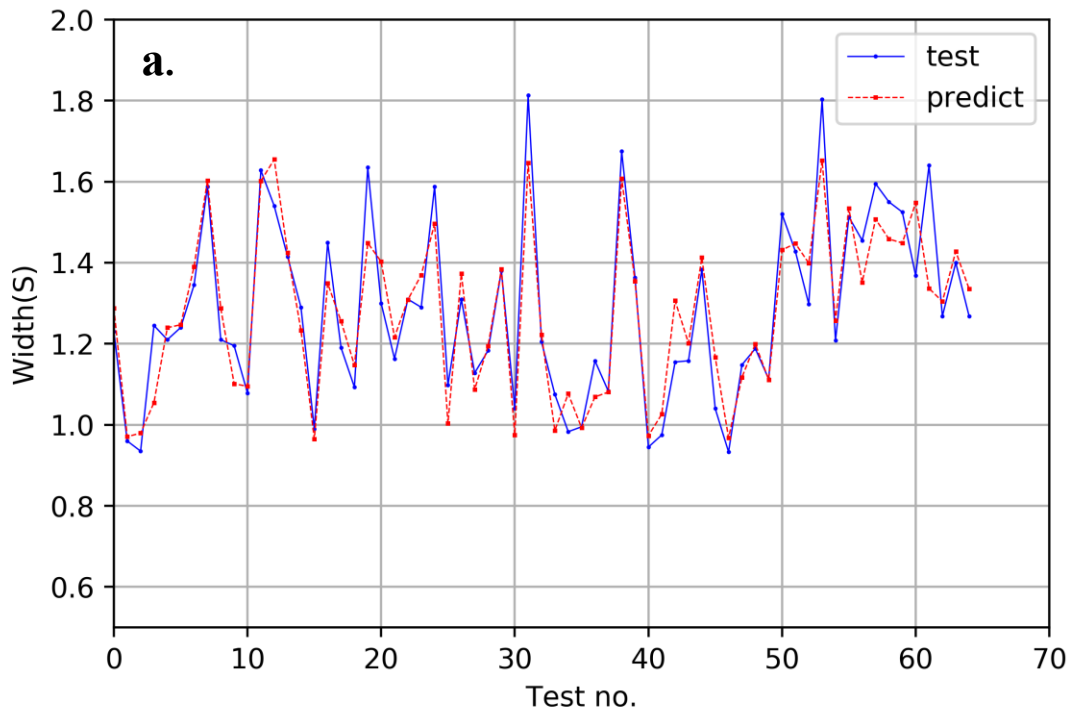


Figure E.2 Plot of single-track width value in (a)ANN and (b)MLR.

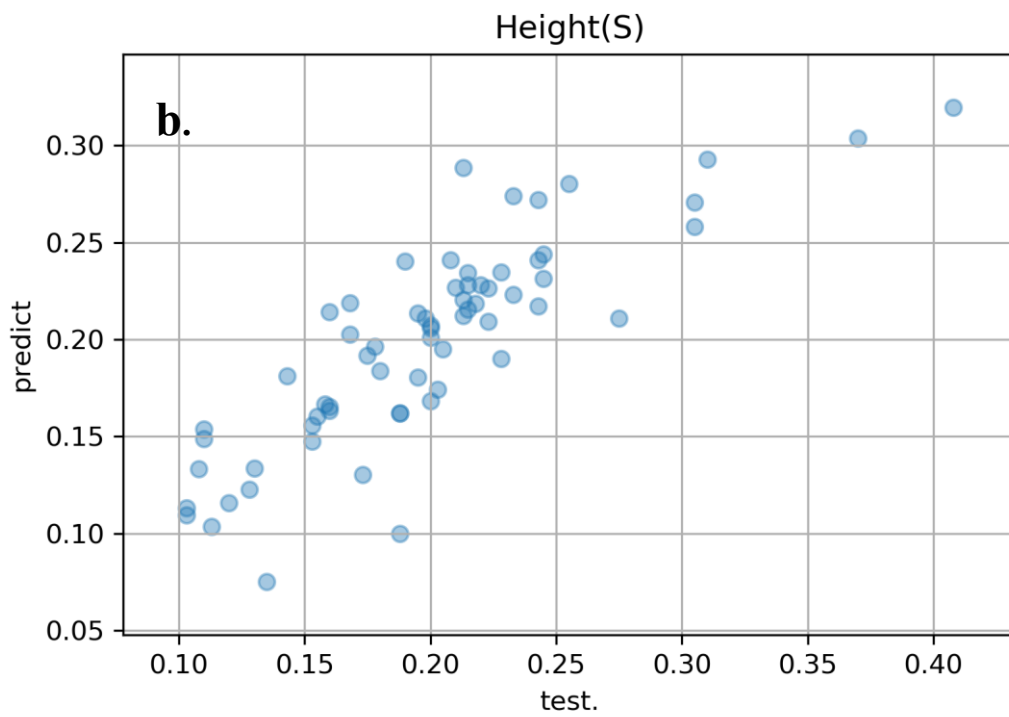
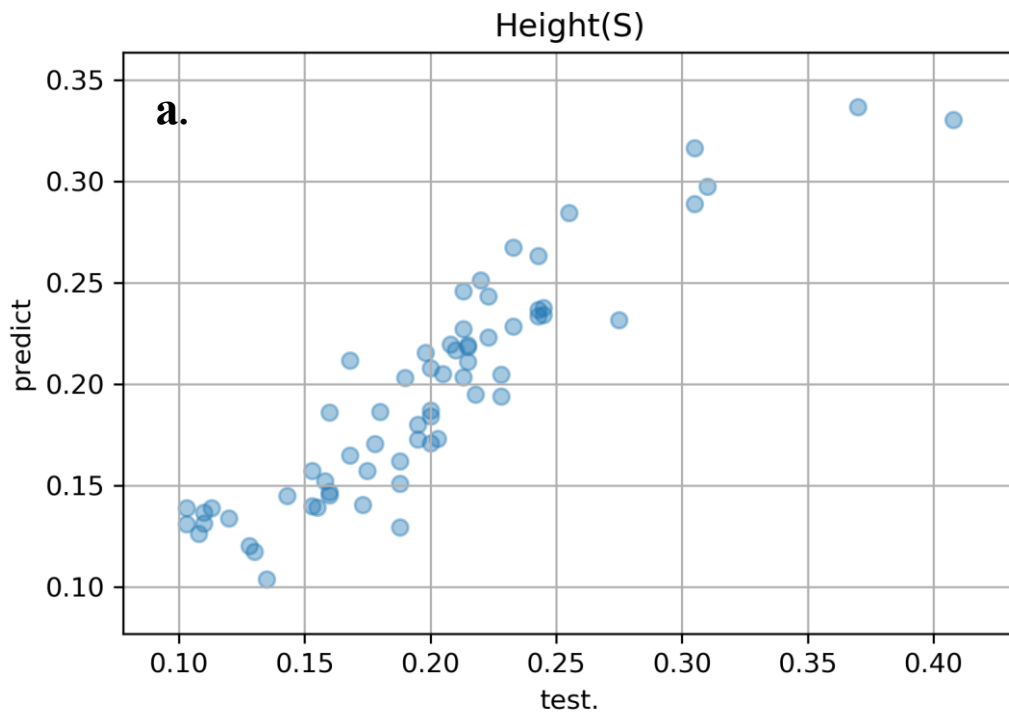


Figure E.3 Plot of single-track height value in (a)ANN and (b)MLR.

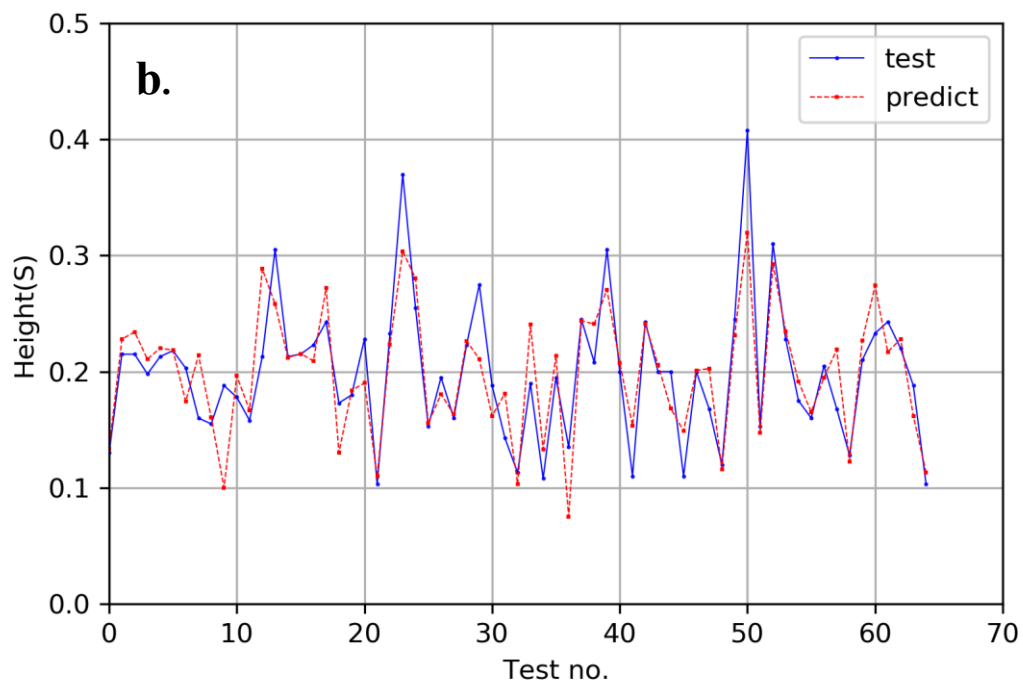
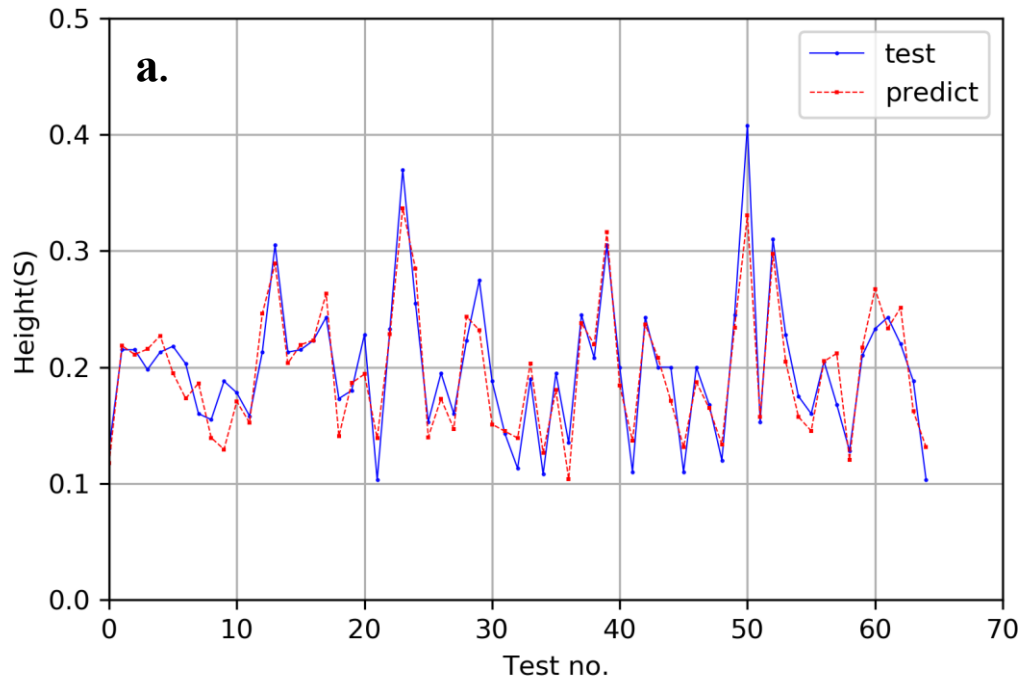


Figure E.4 Scatter of single track height between actual and predicted value in (a)ANN and (b)MLR.

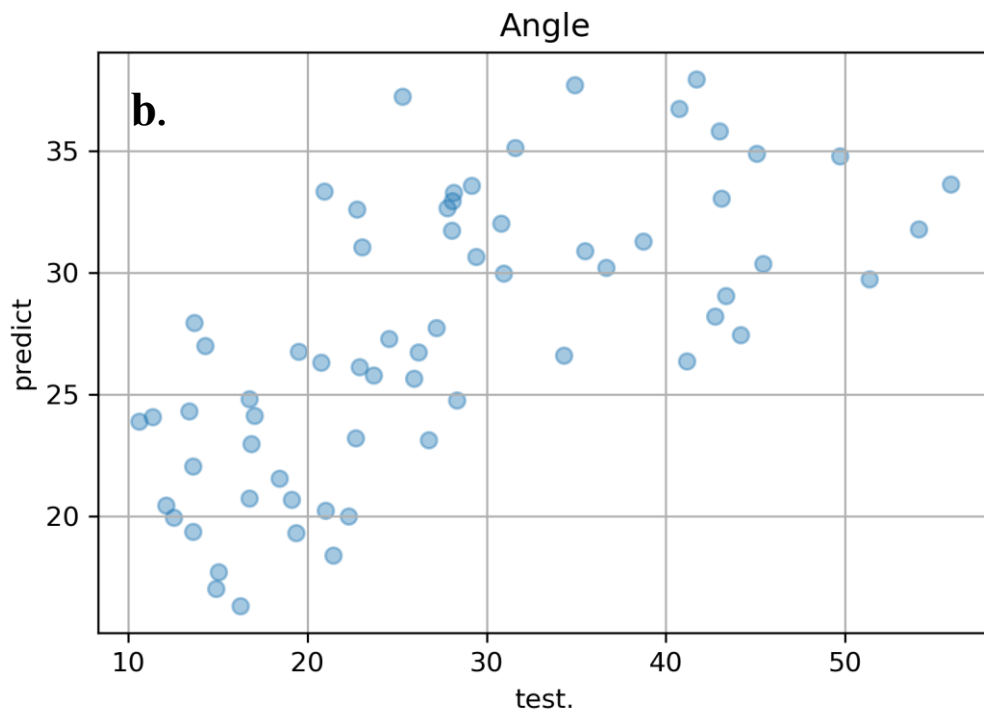
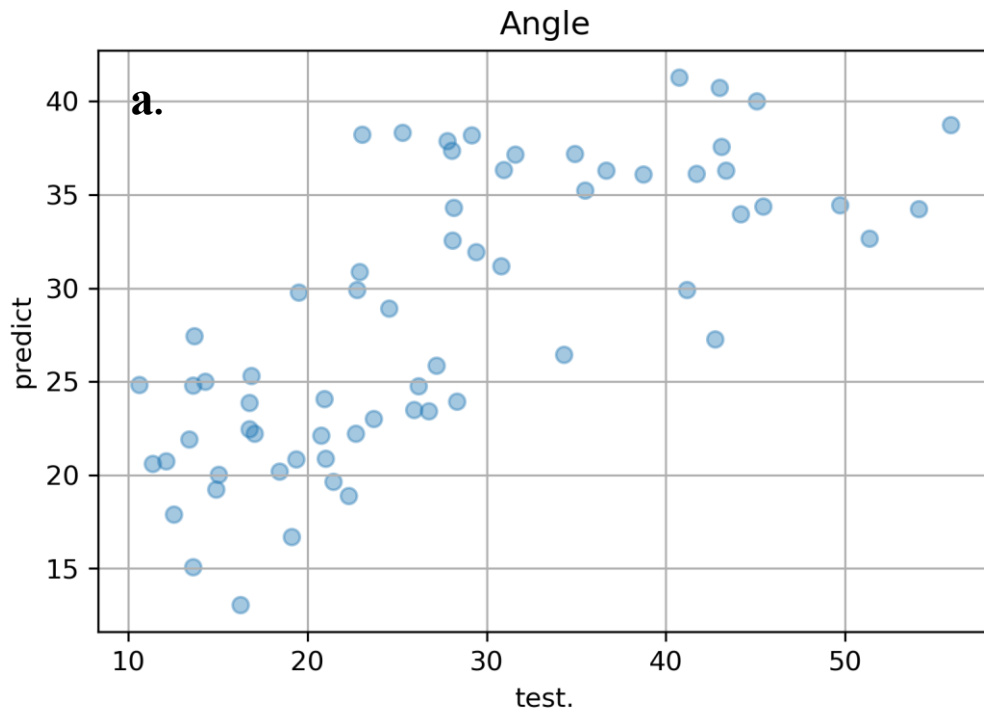


Figure E.5 Plot of single-track angle value in (a)ANN and (b)MLR.

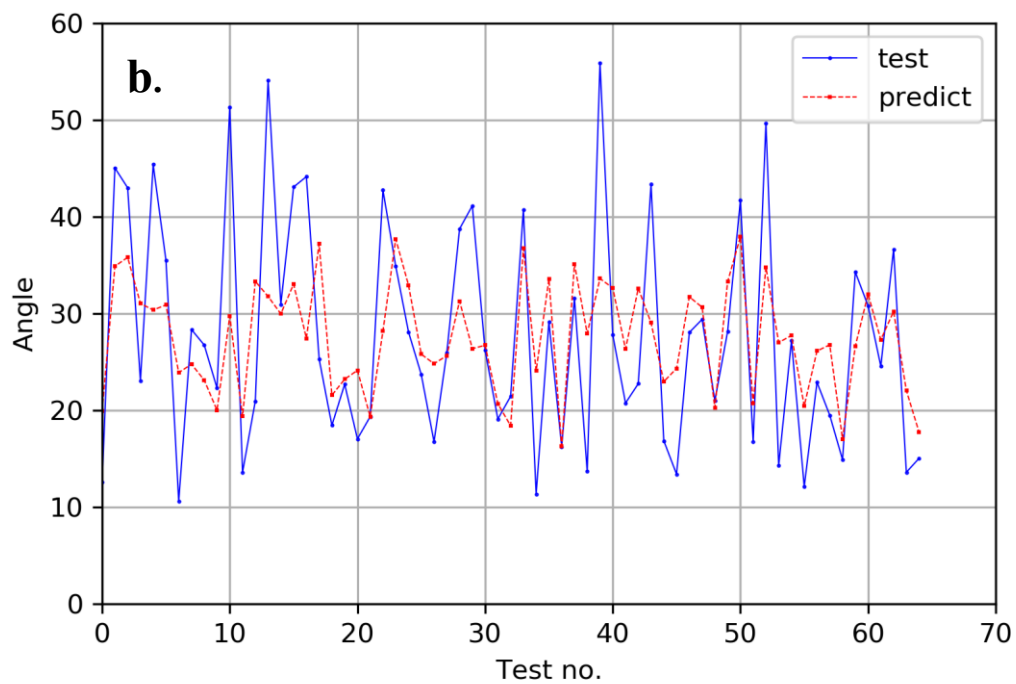
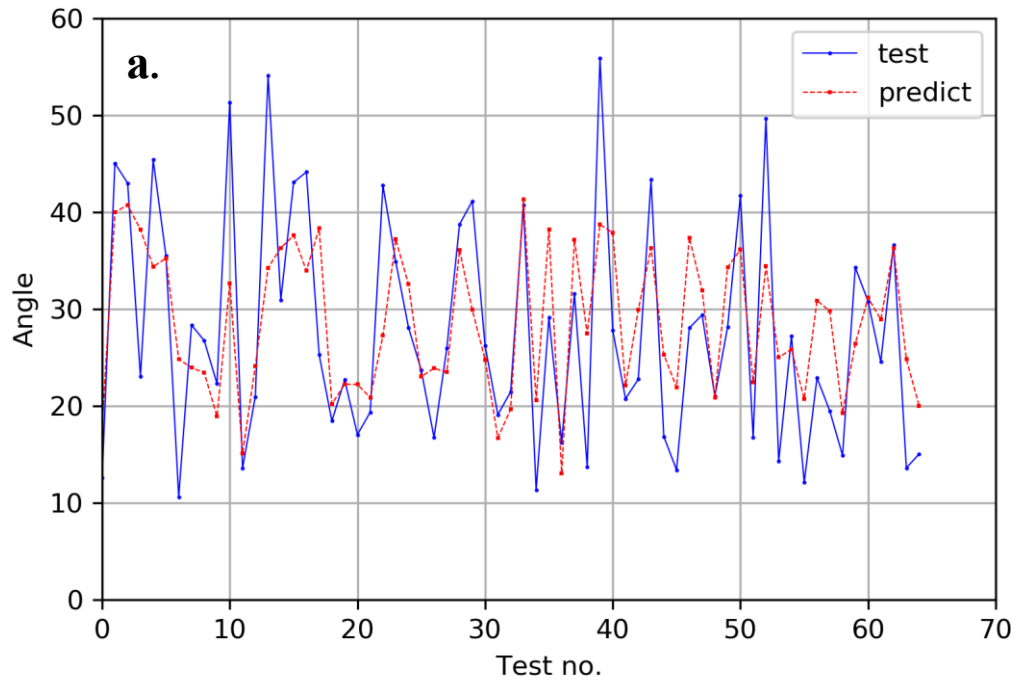


Figure E.6 Scatter of single track angle between actual and predicted value in (a)ANN and (b)MLR.

Acknowledgement

First of all, I would like to express my gratitude to Prof. Namhun Kim, a professor in charge who helped the research with a lot of advice and courage. As a mentor of research, you have helped me to complete my graduate course. Also, I would like to express my gratitude to Professor Sang Hoon Kang and Professor Hyung Wook Park for participating as members of thesis committee.

In particular, Prof. Namhun Kim provided many guides on the Additive Manufacturing field, which was unfamiliar at first, and thanks to the interest and effort of him, I was able to study this subject in detail. Always, I was grateful and honored to learn from Prof. Namhun Kim. In addition, Prof. Sang Hoon Kang and Prof. Hyung Wook Park received many teachings in class and thanked them.

Also, I would like to express my gratitude to the UCIM members. Dr. Eunjoo Park and Dr. Jooyeon Kwon helped with professional knowledge and research methods as researchers. In particular, Dr. Eunjoo Park's advice in related my research has really helped me develop as a researcher. And it was a great happiness for me to be able to study in the lab with Donghwan, Young-gwang, Moise, Jeongsik and Eunseo. Also, I would like to thank Moon-young, Ga-Hyeong, Haekwon, Jageon, Minsoo for sharing various works, competitions, and studies. It's not a long time, but I'm also grateful to Joo-eun who was able to study together for a while. Also, thanks to the 3DAM members.

Lastly, Gu-el Crew members who are Jaehyung, Seungse, Sewon, Jungwoo, Gyujin, and Jihong gave me a lot of support during their graduate school days, and they were able to share many emotions when I was in trouble, joy, and sadness, so I was very grateful to live with them. I really thank Gu-el crew for always supporting me.